

# PCCP

Accepted Manuscript

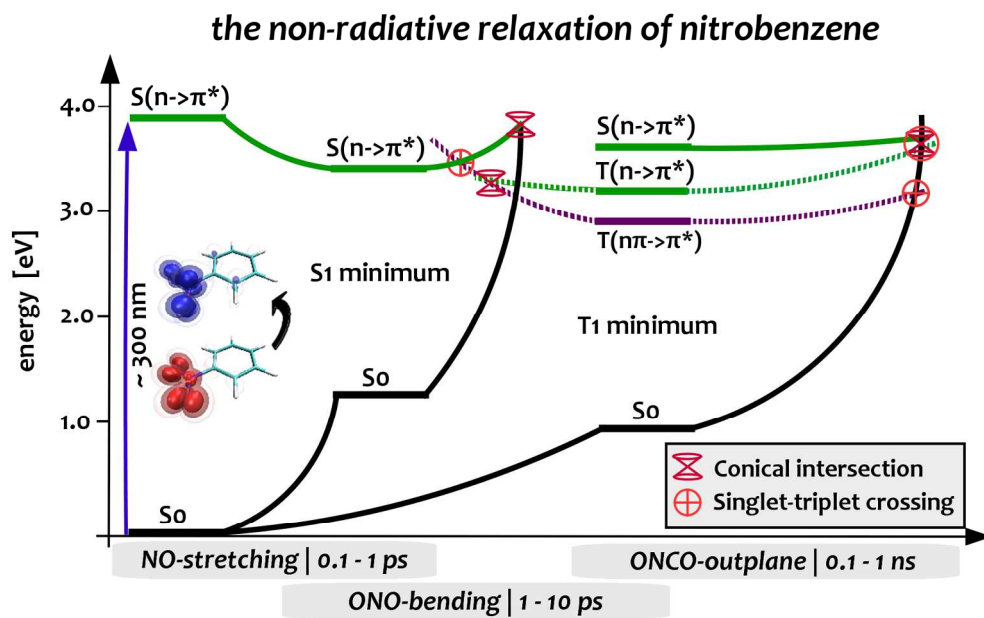


This is an *Accepted Manuscript*, which has been through the Royal Society of Chemistry peer review process and has been accepted for publication.

*Accepted Manuscripts* are published online shortly after acceptance, before technical editing, formatting and proof reading. Using this free service, authors can make their results available to the community, in citable form, before we publish the edited article. We will replace this *Accepted Manuscript* with the edited and formatted *Advance Article* as soon as it is available.

You can find more information about *Accepted Manuscripts* in the [Information for Authors](#).

Please note that technical editing may introduce minor changes to the text and/or graphics, which may alter content. The journal's standard [Terms & Conditions](#) and the [Ethical guidelines](#) still apply. In no event shall the Royal Society of Chemistry be held responsible for any errors or omissions in this *Accepted Manuscript* or any consequences arising from the use of any information it contains.



We present a complete mechanistic picture of the non-radiative relaxation of nitrobenzene via IC and ISC along three internal coordinates.

# On the molecular mechanism of non-radiative decay in nitrobenzene and the unforeseen challenges this simple molecule holds for electronic structure theory

Jan-M. Mewes<sup>a</sup>, Vladimir Jovanović<sup>b</sup>, Christel M. Marian<sup>b</sup> and Andreas Dreuw<sup>a</sup>

Received (in XXX, XXX) Xth XXXXXXXXXX 200X, Accepted Xth XXXXXXXXXX 200X

First published on the web Xth XXXXXXXXXX 200X

DOI: 10.1039/b000000000x

In this work, we present a complete mechanistic picture of the non-radiative decay of the mono-substituted aromatic compound nitrobenzene from the bright singlet state to the electronic ground state. This mechanism involves internal conversion (IC) and inter-system crossing (ISC) along three dominating internal coordinates of the nitro group and consistently explains the experimental findings. Relaxation from the lowest triplet state via ISC occurs along the out-of-plane bending coordinate of the nitro group, while initial IC as well as ultrafast ISC into the triplet manifold take place along symmetric NO stretching and ONO bending modes that have not been considered yet. The proposed mechanism is based on high-level single- and multi-reference electronic structure calculations employing ADC3, MOM-CCSD(T), EOM-CCSD, DFT/MRCI and CAS-SCF/NEVPT2 level of theory, which is, as we will demonstrate, absolutely necessary to assure a reliable and sufficiently accurate theoretical description of nitrobenzene. The need for third-order methods will be traced back to the large double-excitation character of about 50 % of the second excited singlet state of nitrobenzene. As a result, second-order methods like approximate coupled-cluster of second order (CC2) and partially even (EOM-)CCSD yield a qualitatively wrong picture of the excited states. Surprisingly, already the description of the ground state geometries is problematic at the CC2 and partially also CCSD level of theory.

## 1) Introduction

As early as in 1900, Ciamician and Silber first reported on their experiments on light-induced reactivity of various compounds. A large group of these compounds consisted of substituted nitro-aromatics e.g. ortho-nitrobenzaldehyde, which is converted to nitroso-benzoic acid in the presence of UV-light.<sup>1</sup> Since then, nitro-aromatics and their photoreactivity have been investigated in numerous studies and found countless applications as photochemical reagents as well as in photoswitches and photolabile protecting groups.<sup>2,3,4</sup> In particular for the latter applications, a profound knowledge of the character of the ground and low-lying excited states as well as of the very first photophysical processes taking place after excitation is indispensable to allow for rational design of these compounds. In general, the photochemical processes and excited states of nitrobenzene (NB) as the most simple and prototypical nitro-aromatic are of fundamental academic interest. This is reflected by about 10 000 hits obtained by searching for the term “nitrobenzene” in this journal and 180 000 hits with google scholar. There exists, however, neither detailed knowledge along which molecular coordinates of the NB molecule the ultrafast photophysical processes like internal conversion (IC) and inter-system crossing (ISC) take place nor even common agreement on the character of the lowest excited states has been achieved yet.

From an experimental point of view, one of the reasons for this knowledge gap for such a simple molecule is the non-radiative character of almost all photophysical processes in

NB. It is non-fluorescent, non-phosphorescent<sup>5</sup> (other sources report a very weak phosphorescence with a very low quantum yield  $< 10^{-3}$ )<sup>6</sup> and shows only a broad, unstructured excited-state absorption with maxima at 400 and 650 nm.<sup>7</sup> For NB vapor, there is only one strongly absorbing singlet state below 6 eV, which is a  $\pi \rightarrow \pi^*$  excitation at 5.16 eV (240 nm) and two much weaker absorptions, one of which is visible only in the gas-phase spectrum around 4.42 eV (280 nm) and another only evident in solution at approximately 3.8 eV (326 nm).<sup>8</sup>

For practically all theoretical investigations of chemical compounds containing the nitrobenzoic moiety reported so far usually either DFT methods (e.g. B3-LYP/6-31G\*) or perturbative coupled cluster of second order (CC2) have been used,<sup>9,10</sup> which, as we will demonstrate, do not even provide a qualitatively correct description of NB and/or closely related molecules. The coupled-cluster based CC2 predicts an erroneous ground state geometry for NB, which is largely improved with MP2 or DFT/B3-LYP. The latter, however, yields far too low excitation energies for any compound including the nitrobenzoic moiety and electron donating groups, which is due to the well known charge-transfer error of TD-DFT.<sup>11</sup> In fact, most ortho-nitrobenzylidene photolabile protecting groups do contain additional electron donation groups such as e.g. 4,5-dimethoxy substituents or alpha-carboxy groups, which have the purpose to shift the absorption to longer wavelength and increase solubility in water.

The difficulties determining the character of the lowest

excited triplet state of NB most certainly result from the fact that there are two or three low-lying states with similar energy that require a balanced description of local  $n \rightarrow \pi^*$ , local  $\pi \rightarrow \pi^*$  and charge-transfer character, which are in addition differently influenced by solvation. Moreover, the relative energies of these states strongly depend on the geometrical parameters such as the NO bond length and ONO bending angle. In particular the computed values of these parameters exhibit large deviations from the experimental ones even at high coupled-cluster level of theory (see section 4, ground state equilibrium geometry).

In this work, we attempt to shed light on the photophysical and photochemical processes of NB, which is the smallest representative for nitroaromatic compounds. Due to its small size and high  $C_{2v}$  symmetry, even highest level single- and multi-reference ab-initio calculations (ADC3, CCSD(T), CAS(14/11)) with reasonably large basis sets (def2-TZVP, cc-pVTZ) are feasible. This allows for a thorough investigation of the character of the lowest triplet state, which is of utmost importance for the non-radiative decay processes in NB.

In an attempt to make this paper accessible for theoreticians as well as experimentalists, the theoretical details of the somewhat extensive search for a suitable methodology are collected in section 4. Readers that are mainly interested in the mechanism of non-radiative relaxation of NB will find a short summary of electronic structure of NB ground and excited states in section 3 and may skip section 4 to continue with section 5, which covers mechanistic aspects of non-radiative decay.

In general, this paper is arranged as follows: in **section two**, a short summary of existing experimental and theoretical literature will be given to create a starting point for our investigation. In **section three** the relevant singlet and triplet excited states of NB will be characterized and summarized foreclosing the conclusion from section four. In **section four**, results, accuracy and reliability of various methods (CIS, CIS(D), CC2, CCSD, EOM-CCSD, ADC2, ADC3, DFT/MRCI, CAS-SCF/NEVPT2 and MOM-CCSD(T)) for ground and excited states will be discussed in detail to explain problems concerning theoretical description of NB. At the end of section four, technical details of programs and methods are summarized. In **section five**, the relevant internal coordinates of the NB molecule will be investigated regarding possible pathways for non-radiative relaxation processes based on relaxed potential-energy-surface scans along ONO bending, symmetric NO stretching and ONCO out-of-plane bending coordinates calculated at the ADC3 and DFT/MRCI level of theory.

## 2) Previous experimental and theoretical investigations

The very first photochemical experiments on NB and nitroaromatic compounds were conducted by Ciamician and Silber in the beginning of the 20th century. For their investigations, they exposed solutions of NB and various ortho-substituted nitro-aromatics (e.g. o-nitrotoluene, o-nitrobenzaldehyde) to sunlight over long periods of time (days to years).<sup>1</sup> Thereby, they discovered the photooxidative

reactivity of the nitro group with respect to neighboring substituents and also solvent molecules.

After investigating the vapor-phase photochemistry of NB, Hurley and Testa were the first to infer that hydrogen-abstraction by the electronically excited nitro group may be a key step in the manifold photochemistry of nitrobenzyl compounds.<sup>6</sup> In the same work, they also found that ISC plays a crucial role in NB photochemistry. By means of quenching experiments, they determined the triplet yield to be as big as  $67 \pm 10\%$ . Moreover, they concluded that the strong concentration dependence of many photochemical reactions of NB in solution has to be a result of an unusually short lifetime of the triplet of NB compared to other nitro aromatics and does not originate from a low triplet yield. From their experiments, they suggested a triplet lifetime  $< 1$  nanosecond, which was, as it turned out later (see below), a very good estimate.

To determine the character of the NB excited state responsible for the experimental absorption peak around 5.1 eV, Nagakura et al. recorded an absorption spectrum of NB vapour and in various solvents of increasing polarity.<sup>8</sup> In combination with very basic molecular-orbital theory considerations, they suggested the strongly absorbing singlet state at 5.16 eV to be a charge-transfer (CT) state of  $A_1$  symmetry, in which an electron is transferred from the benzene ring to the nitro group. Another weakly absorbing state that is found at about 3.8 eV was suggested to be the lowest  $n \rightarrow \pi^*$  excitation because of its solvatochromatic blue shift. Although this state is symmetry forbidden at the strictly  $C_{2v}$  symmetric ground state equilibrium geometry, it can gain an oscillator strength ( $f_{osc}$ ) of 0.02 when the symmetry is broken for example by thermal tilting of the nitro group with respect to the benzene ring. The weak absorption exhibiting vibrational fine structure at around 4.42 eV, which is observed only in the gas-phase spectra, was attributed to the  $1B_1$   $\pi \rightarrow \pi^*$  excited-state by comparison to a peak with similar vibrational structure observed for benzene.<sup>11</sup>

To investigate the gas-phase structure of NB, Domenicano et al. carried out electron diffraction experiments on NB vapor.<sup>12</sup> According to these experiments, the geometry is planar but due to a low rotational barrier, the nitro group carries out a large amplitude-tilting motion, causing the unsigned average tilting angle (CCNO dihedral) in the gas phase at 300 K to be about  $13^\circ$ . The critical NO bond-length is  $(122.3 \pm 0.3)$  pm, the CN bond-length is  $(148.6 \pm 0.4)$  pm and the ONO-angle  $(125.3 \pm 0.2)^\circ$ .

Later, Takezaki et al. investigated the relaxation of UV excited NB by means of photoacoustic spectroscopy.<sup>5</sup> The latter allows to detect the changes in optical density caused by temperature change in the molecular environment during the non-radiative relaxation processes. They calculated the triplet yield to be  $(80 \pm 4)\%$ , which is slightly higher than the one reported by Hurley and Testa. Furthermore, due to the high time resolution of the photoacoustic transient grating and population grating techniques employed, they were able to determine an upper limit for the timescale of the fastest process of 100 fs as well as the timescale of ISC into the triplet manifold to be 6 ps.<sup>13</sup> They found the triplet population to decay in the nanosecond time regime (i.e. 480-900 ps

lifetime depending on solvent and temperature) to give back ground state NB. Surprisingly, the lifetime of the triplet hardly depends on solvent polarity, but rather on the chain length of the alkane solvent and temperature. A lower bound for the energy of the relaxed triplet state was determined to be at 2.55 eV by quenching experiments. Based on preliminary CAS-SCF calculations, they suggested the IC and ISC processes to take place along the ONCO out-of-plane coordinate of the nitro group (figure 2 in ref 13). For the CAS-SCF investigation of NB, they used a small basis set with polarization functions only on the nitrogen atom and a small active space.<sup>14</sup> Although they find similar ordering and character of the lowest excited states, the energies they report are too low by about 1 eV compared to the experiment.

J. Quenneville et al. investigated the photochemical processes in NB theoretically by means of quantum-chemical calculations employing a mixture of MRQDPT, CAS-SCF and TD-DFT.<sup>15</sup> They optimized the  $S_1/S_0$  conical intersection (CI) using CAS-SCF yielding a geometry that is, apart from the tilting angle of the nitro group also found in this work (intersection of  $S_1$  and ground state in figure 8). Based on this result, they suggested the internal conversion to take place along this ONCO out-of-plane and CCNO dihedral coordinate.

### 3) Ground and excited states of nitrobenzene

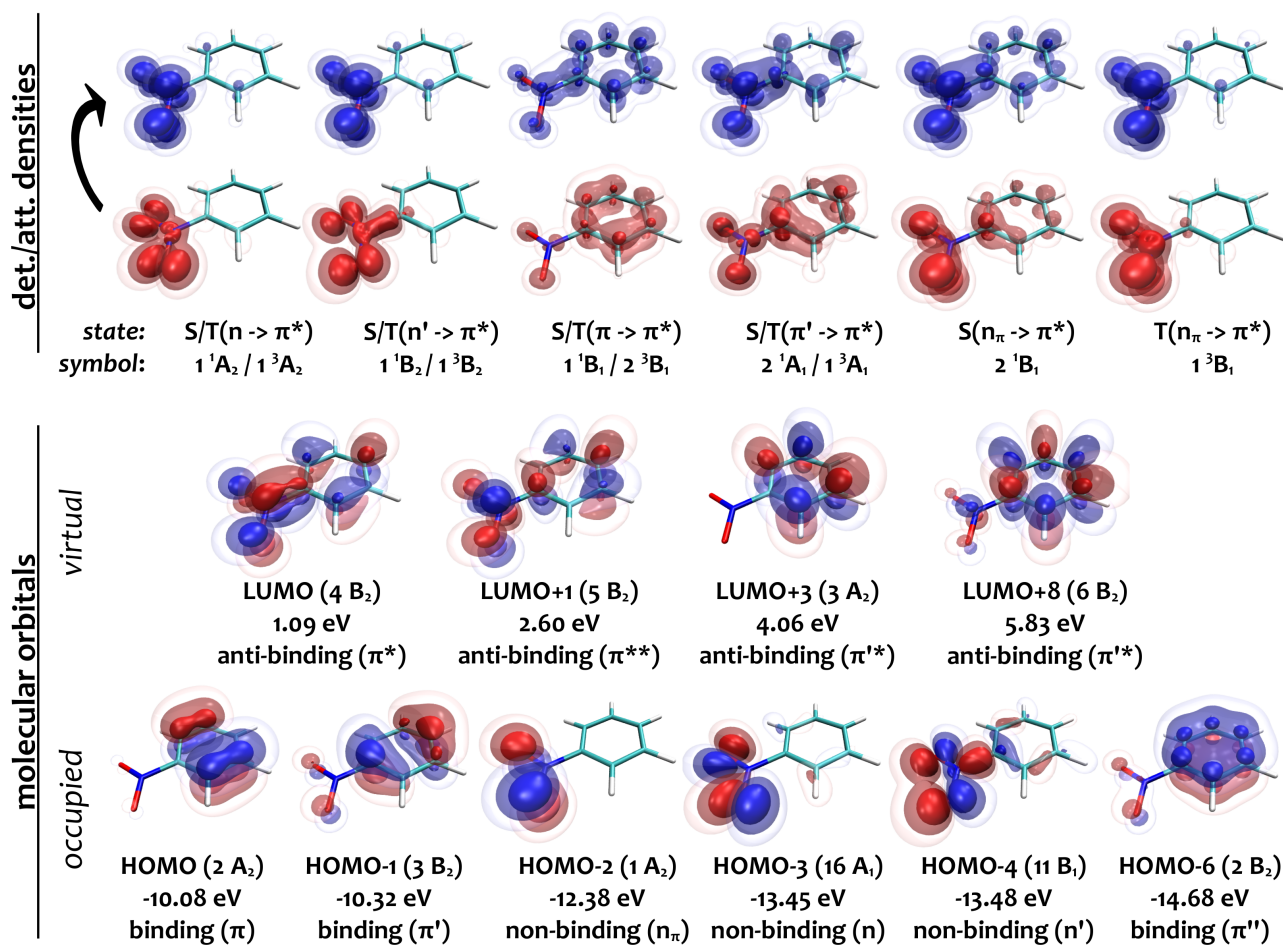


**Figure 1** Isosurfaces for attachment (top, blue) and detachment (top, red) densities for the energetically lowest excited singlet states and the  $n_\pi \rightarrow \pi^*$  triplet state at the ADC3 level of theory as well as the relevant molecular orbitals (bottom) of nitrobenzene calculated with the def2-TZVP basis for the B2-PLYP/def2-TZVP geometry. For all states apart from the  $n_\pi \rightarrow \pi^*$  state, attachment and detachment densities of singlet and respective triplet states are hardly distinguishable. The isosurfaces were rendered with the isovalues 0.018 (opaque), 0.006 (colored transparent) and 0.002 (transparent) for the att./det. densities and 0.1, 0.05 and 0.025 for the orbitals. The use of three surfaces instead of only one allows oneself to distinguish between major contributions (opaque surfaces) and minor ones and furthermore to estimate the gradient of the density from the distance of the three surfaces.

### Singlet excited states

According to our calculations, the lowest excited singlet state with large oscillator strength ( $f_{osc}$ ) of about 0.25 is a  $\pi \rightarrow \pi^*$  excited state with CT-character as suggested by Nagakura et al.<sup>8</sup> Since this bright state with the same symmetry as the ground state ( $A_1$ ) is characterized by an excitation from the second highest occupied  $\pi$  orbital (HOMO-1), it will be referred to as  $S(\pi' \rightarrow \pi^*)$  state. Like for all excited states discussed here, the biggest components of the excitation vector of the  $S(\pi' \rightarrow \pi^*)$  state are excitations to the LUMO, which is a mixture of mainly the  $\pi^*$  orbital at the nitro group with significant contributions from a benzene  $\pi^*$  orbital. For the rather local  $n \rightarrow \pi^*$ ,  $n' \rightarrow \pi^*$  and  $n_\pi \rightarrow \pi^*$  states (see attachment/detachment densities in figure 1), excitations to the LUMO+1 are included in the excitation vector as well, but with the opposite sign. Eventually, the contributions from LUMO and (inverse) LUMO+1 cancel out at the carbon atoms while they add up at the nitro group, yielding the locally excited states.

At the Franck-Condon (FC) point there are four dark singlet excited states energetically below the bright  $\pi' \rightarrow \pi^*$  excited state. These include two  $n \rightarrow \pi^*$  and two  $\pi \rightarrow \pi^*$  excited states, which will be termed  $S(n \rightarrow \pi^*)$  (term symbol:  $1^1A_2$ , main contribution from the HOMO-3),  $S(n' \rightarrow \pi^*)$  ( $1^1B_2$ , HOMO-4),  $S(\pi \rightarrow \pi^*)$  ( $1^1B_1$ , HOMO) and  $S(n_\pi \rightarrow \pi^*)$  ( $2^1B_1$ , HOMO-2). The latter state is termed  $S(n_\pi \rightarrow \pi^*)$  because it is involving the HOMO-2, which is a non-bonding orbital of  $\pi$ -symmetry located at the nitro group. The excitation vector of this state exhibits large contribution from double excitations (see figure 2). Therefore, the energy of this state is significantly overestimated by any linear-response (LR) method. Since this is not the case for the corresponding triplet state, which is largely dominated by single electron excitations, one obtains a huge, artificial singlet-triplet splitting of 2-3 eV with any LR or second order method. Eventually, this state will turn out to be essential for the photochemistry of NB, which complicates the investigation since any accurate and reliable theoretical description of an

excited state with significant double excitation character requires a reasonable description of doubly excited states.

The  $1 B_1 S(\pi \rightarrow \pi^*)$  state is characterized exclusively by the HOMO  $\rightarrow$  LUMO excitation exhibiting very limited *fosc*. The  $1 B_2 S(n' \rightarrow \pi^*)$  is located at the nitro group and also dark. These  $S(n' \rightarrow \pi^*)$  and  $S(\pi \rightarrow \pi^*)$  states are of limited relevance for NB photochemistry as they cannot become the lowest excited states but rather play a role as intermediate ladder steps during IC in the singlet manifold.

The lowest  $1 A_2 S(n \rightarrow \pi^*)$  excited state is strictly localized at the nitro group. It can obtain little but significant *fosc* of about 0.02 if the nitro group is tilted with respect to the aromatic ring and hence shows up in the experimental spectrum recorded in solution at  $T = 300$  K as a small shoulder at about 3.8 eV.

### Triplet states

In the triplet manifold, three excited states have a similar energy and may thus become photochemically relevant. Concluding the results of all our calculations for unsubstituted NB in vacuum, the lowest triplet state at the ground state equilibrium structure is most likely the  $T(n_\pi \rightarrow \pi^*)$  state, whereas the  $T(n \rightarrow \pi^*)$  and  $T(\pi' \rightarrow \pi^*)$  states are only little higher in energy ( $\sim 0.2$ - $0.5$  eV depending on the method, for a detailed analysis see section 4).

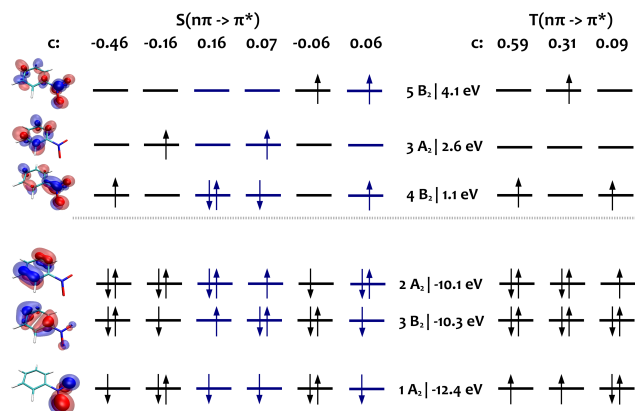


**Figure 2:** Composition of the  $n_\pi \rightarrow \pi^*$  excited singlet and triplet states ADC3/def2-TZVP//B2-PLYP/def2-TZVP level of theory.

Doubly excited determinants are shown in blue. Over-all, they make up for about 50 % of the contributions to the excitation vector of this state.

In contrast to its singlet analogue, the  $1 B_1 T(n_\pi \rightarrow \pi^*)$  state is characterized mainly by single-electron transitions, the largest of which is originating from the HOMO-2 (figure 2). Surprisingly, this does not eliminate the problems concerning the accuracy of its theoretical description. Even for this  $T(n_\pi \rightarrow \pi^*)$  state, at least EOM-CCSD level of theory is required to obtain a qualitatively correct picture in agreement with higher order single-reference and multi-reference methods such as ADC3 and MOM-CCSD(T), whereas CC2 as well as all second order methods yield a wrong order of the lowest triplet states (i.e.  $n \rightarrow \pi^*$  far below  $n_\pi \rightarrow \pi^*$ ). This becomes even more evident from the magnitude of the triples correction to MOM-CCSD, which is about 0.3 eV for this

state (singlet  $-0.3$  eV and triplet  $+0.3$  eV), while for most other states its well below 0.1 eV (see figure 4, bright and dark blue bars).

The analogue of the lowest  $1 A_2$  singlet, the  $T(n \rightarrow \pi^*)$  state, is the second lowest triplet state at the FC point. A key property of these lowest triplet states is the different position of their respective minima along the ONO bending coordinate (see table 1), which causes the singlet and triplet  $n \rightarrow \pi^*$  states to intersect with  $T(n_\pi \rightarrow \pi^*)$  state at small ONO bending angles. For even smaller ONO angles, these states also cross the ground state surface (see figure 7). These seams and crossings between the  $T(n_\pi \rightarrow \pi^*)$  and  $T(n \rightarrow \pi^*)$  states along the ONO bending coordinate will turn out to be of great importance for the IC and ISC processes in UV excited NB.

If a very polar solvent is present, also the  $1 A_1 T(\pi' \rightarrow \pi^*)$  state can become the global energy minimum of the triplet manifold due to its CT character. Although this is presumably impossible for NB, it becomes feasible if substituents with +m effect are introduced in the meta and/or para positions. Practical examples are 4,5-dimethoxy-ortho-nitrobenzylcaged compounds, for which it is well established that the triplet population can be trapped in a long-lived triplet state under these conditions, reducing the quantum yield for the uncaging reaction from around 10 % to 1-2 %.<sup>9,16,17</sup> Here, the initial hydrogen abstraction that has been shown to take place in the singlet and triplet  $n \rightarrow \pi^*$  states, is prevented by trapping the population in the low lying  $T(\pi' \rightarrow \pi^*)$  minimum.<sup>18,10</sup>

For a more detailed analysis of the energetics of the lowest triplet states explicitly discussing the results of various single- and multireference methods the reader is referred to section 4.

### Inter-system crossing

For NB, the probability of transitions between singlet and triplet states via spin-orbit coupling (SOC) can be derived qualitatively from El-Sayed's rules.<sup>19</sup> According to the latter, ISC is fast between states involving orbitals of different symmetry, e.g.  $n \rightarrow \pi^*$  to  $\pi \rightarrow \pi^*$ , while it is slow between states of the same orbital symmetry. Hence, concerning NB, it may be concluded that ISC takes place between the lowest  $S(n \rightarrow \pi^*)$  and  $T(n_\pi \rightarrow \pi^*)$  states, while the ISC rates between  $n \rightarrow \pi^*$  singlet and triplet states should be three orders of magnitude smaller. This qualitative picture is substantiated by DFT/MRCI and CAS-SCF/NEVPT2 calculations of SOC, which are around 100 /cm between  $S(n \rightarrow \pi^*)$  and  $T(n_\pi \rightarrow \pi^*)$  states and exactly zero between the states of same symmetry at the  $C_{2v}$  symmetric ground state equilibrium structure. For ISC from the triplet manifold back to the ground state the same rules apply and consequently, SOC is large between  $n \rightarrow \pi^*$  excited states and the ground state, while for  $\pi \rightarrow \pi^*$  or  $n_\pi \rightarrow \pi^*$  states SOC with the singlet ground state vanishes. This, however, changes when the molecule is distorted out of its  $C_{2v}$  symmetry. Along the ONCO out-of-plane coordinate for example, the SOC of the  $T(n_\pi \rightarrow \pi^*)$  state with ground state increases to 65 /cm at an ONCO out-of-plane angle of  $40^\circ$  ( $T(n_\pi \rightarrow \pi^*)$  relaxed structure), while the SOC between  $T(n \rightarrow \pi^*)$  and the ground state is reduced to 15 /cm (see figure 8).

## 4) Results, methodology and accuracy

### Ground state equilibrium geometry

During our theoretical investigation of NB using the approximate coupled cluster theory of second order (CC2), this method was found to predict a ground state geometry that is significantly different from the experimental vapor geometry. The most substantial deviation is observed for the NO bond length, which is 122.3 pm in the experiment compared to 124.6 pm at the CC2/def2-TZVP level of theory. At first glance, this deviation of 2.3 pm seems negligible and is inconspicuous due to a fortuitous error compensation between the CC2 geometry and linear-response (LR)-CC2 excitation energies, which are actually much closer to experimental values for the faulty geometry. Surprisingly, CCSD/def2-TZVP and CCSD/cc-pVTZ do not perform much better as they overcompensate the error, both yielding a bond length of 121.5 pm, which is significantly too short compared to the experiment. If one compares excitation energies calculated for ground state geometries obtained with CC2 and CCSD, the impact of this erroneous bond length becomes evident: Since CC2 and CCSD deviate in opposite directions, the differences add up and the excitation energies of some of the states differ by as much as 0.5 eV. The reason is that between 120 pm and 125 pm, the vertical excitation energies of the excited states localized at the nitro group are extremely sensitive with respect to this bond length and are shifted by as much as 0.13 eV/pm (see figure 6), while the other excited states are hardly affected. Due to the state-dependent shift, the use of the CC2 ground state geometry introduces a systematic error not only to absolute, but also to relative state energies in the order of 0.25-0.3 eV with respect to the experimental geometry.

The agreement between experimental structure and CCSD may be improved by using the smaller double zeta SVP or cc-pVDZ basis sets yielding 122.1 pm, which is at least within the error bars of the experiment. Further investigating this issue, it was found that simple MP2, SCS-MP2 and double-hybrid DFT/B2-PLYP in combination with the def2-TZVP basis set yield NO bond lengths of 122.7 pm, 122.6 pm and 122.5 pm, respectively. In particular B2-PLYP shows an extremely good agreement with experimental data considering other structural parameters such as ONO angle and CC bond lengths as well as excitation energies, whereas the calculations take a small fraction of the computational resources required for CCSD. Therefore, we decided to use the B2-PLYP geometry as basis for the rigid scans as well as vertical excitation energy calculations.

### Excited states of nitrobenzene

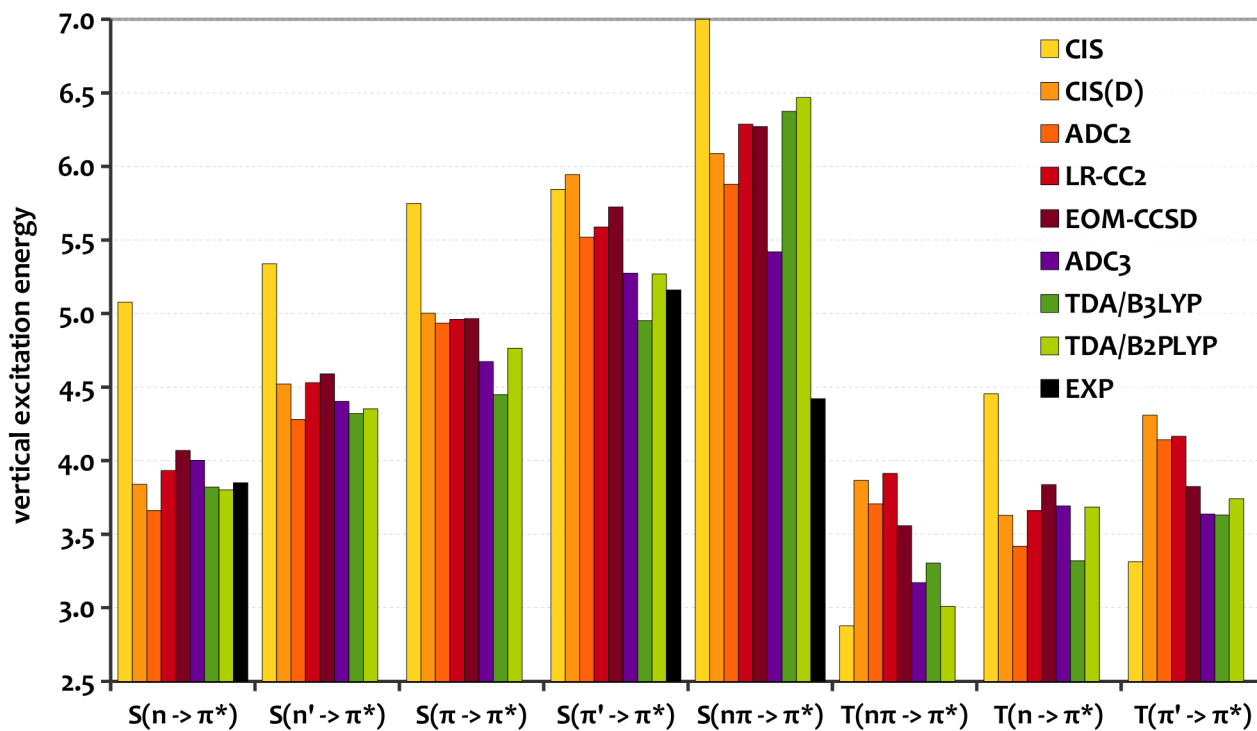


**Figure 3:** Plot of the vertical excitation energies calculated with single-reference methods of increasing accuracy. The level of theory increases from yellow (first order) over red (second order) to purple (third order), DFT results are green. Regarding the states for which experimental data is available, ADC3 outperforms EOM-CCSD. For the  $S(n \rightarrow \pi^*)$  excited state, ADC3 yields excitation energies that are little too high and ADC2 is superior. All calculation were carried out for the B2-PLYP/def2-TZVP equilibrium geometry with the def2-TZVP basis set.

The quality of the theoretical description of NB is remarkably different for each of the lowest five excited electronic states. Therefore, we used a large variety of methods to calculate vertical excitation energies from CIS through MOM-CCSD(T) as well as various multi-reference methods and DFT to allow for an estimation of trends and to investigate the convergence of the results with respect to the level of theory. Furthermore, our results may help guide the choice of methods for future studies of molecules containing the nitrobenzylic moiety. For reasons of clarity, we will first discuss the results of the single-reference excited state methods (figure 3) and afterwards the results of the multi-reference methods DFT/MRCI and CAS-SCF and finally the calculations employing the maximum-overlap method (MOM) in combination with CCSD(T) (figure 4).

For all states discussed below except the  $n_\pi \rightarrow \pi^*$  singlet and triplet and partially also the  $S(\pi' \rightarrow \pi^*)$  state, the calculated vertical excitation energies are virtually converged at CIS(D) level of theory. CC2, EOM-CCSD, ADC2 and ADC3 and B2-PLYP give results within 0.3 eV as can be seen in figure 3. For the afore-mentioned  $n_\pi \rightarrow \pi^*$  state, however, this agreement breaks down as ADC3 predicts an excitation energy significantly lower than any other method. Even TDA/B2-PLYP, which is within 0.1 eV from the ADC3 result for any other state, gives a much higher energy for the  $S(n_\pi \rightarrow \pi^*)$  state. Foreclosing the result of MOM-CCSD(T) (figure 4), one finds that the excitation energy of this state is actually even lower at this highest level of theory and with 4.42 eV more than 1 eV below the ADC3 result. Although the

$n_\pi \rightarrow \pi^*$  singlet state is of limited relevance for the processes investigated in this work, the corresponding  $T(n_\pi \rightarrow \pi^*)$  state is supposedly the global minimum of the triplet manifold. Therefore, a reliable and accurate description of the  $T(n_\pi \rightarrow \pi^*)$  state and the neighboring  $T(n \rightarrow \pi^*)$  and  $T(\pi' \rightarrow \pi^*)$  states is the key to understanding the non-radiative relaxation processes of NB. But despite the fact that the  $T(n_\pi \rightarrow \pi^*)$  state exhibits no double-excitation character like its singlet analogue, its description is comparably problematic with the single-reference methods being spread over almost 1 eV and the triples correction to MOM-CCSD amounting to 0.3 eV. As a result, the ordering of the lowest triplet states changes multiple times when going from CIS to the approximate second order methods (CIS(D), ADC2, CC2) and

once more regarding EOM/MOM-CCSD and ADC3 and DFT.

To clarify this matter, additional calculations were carried out with methods known to yield a good description of states with double-excitation and/or multi-reference character. These are DFT/MRCI and state-averaged (SA) CAS-SCF/NEVPT2 to investigate the multi-reference character as well as the maximum-overlap method (MOM) in combination with CCSD and CCSD(T) (MOM-CCSD, MOM-CCSD(T)) to obtain a converged description of the doubly excited  $S(n_{\pi} \rightarrow \pi^*)$  state.

#### DFT/MRCI

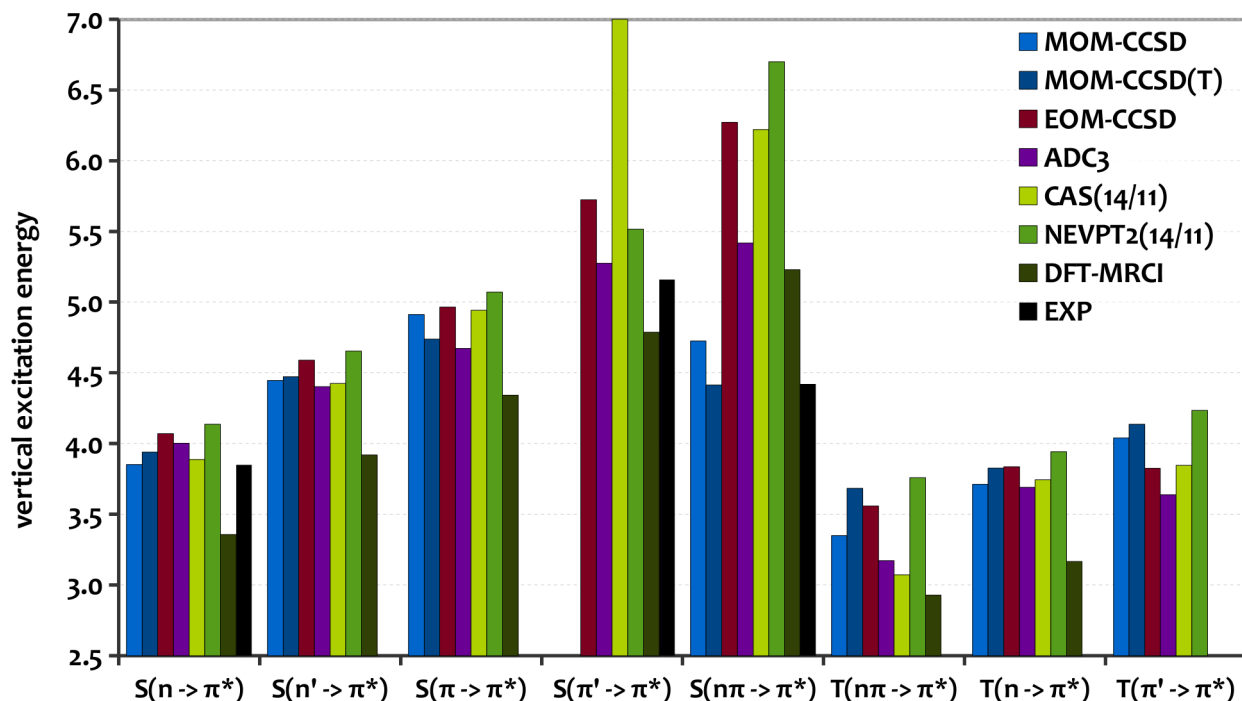


**Figure 4:** Vertical excitation energies calculated with the maximum-overlap method in combination with CCSD/CCSD(T) as well as DFT/MRCI and CAS-SCF/NEVPT2 for the B2-PLYP/def2-TZVP equilibrium geometry. While all methods shown here predict the  $T(n_{\pi} \rightarrow \pi^*)$  state is the lowest triplet state, the critical energy gap to the next higher  $T(n \rightarrow \pi^*)$  state varies from 0.13 eV (MOM-CCSD(T)) to 0.72 eV (NEVPT2) with ADC3 (0.52 eV) and EOM-CCSD (0.3 eV) in between.

Unfortunately, the results of DFT/MRCI suffer from admixture of low-lying doubly-excited intruder states with four open shells, which artificially lower the energy of the physical excited states (see figure 4). Although this is a known problem of DFT/MRCI, it seems to be particularly pronounced in the case of NB and especially the  $S(n \rightarrow \pi^*)$  excited state. An explanation might be the fact that there are indeed low-lying excited states with large double excitation character. Nevertheless, the results of the DFT/MRCI calculations allow for a qualitative comparison of relative energies. Compared to ADC3, the ordering of the states is the same and especially for the  $S(n_{\pi} \rightarrow \pi^*)$  state DFT/MRCI agrees with ADC3. In particular for the difference between the two lowest triplet states DFT/MRCI and ADC3 agree quite well.

#### CAS-SCF

To obtain an initial guess for the CAS-SCF calculation,

MP2/def2-TZVP natural orbitals were generated and reordered according to the choice for the active space (AS) (see below). Concerning the look of their isovalue surface plots, the final CAS-SCF orbitals are virtually indistinguishable from the MP2 natural orbitals and the HF MOs shown in figure 1.

The CAS-SCF calculations were carried out using three different choices for the AS: The largest AS consists of 14 electrons in 11 orbitals (CAS(14/11)), which includes all ten orbitals shown in figure 1 and additionally the lowest bonding  $\pi$ -orbital of the nitro group (lowest orbital of  $B_2$  symmetry, -19.56 eV). This largest AS includes all orbitals with  $\pi$  symmetry as well as all n-orbitals of the nitro group, which should allow for a reasonable description of primary relaxation effects already at the CAS-SCF level of theory. To systematically investigate the importance of each of these orbitals for the relaxation effects, we successively reduced the AS. For the next smaller AS including 12 electrons in 10

orbitals, the  $\pi$ -orbital at the nitro group was removed from the AS. Finally, also the highest and lowest  $\pi$ - and  $\pi^*$ -orbitals of the benzene ring were removed to obtain a CAS(10/8), which only includes orbitals primarily involved in the excitations. In all cases, state-averaging (SA) was done over all states discussed above with equal weights for each. To quantify the influence of the SA scheme, the weights were varied by shifting them either more to the localized  $n \rightarrow \pi^*$  excited states of the nitro group or to the  $\pi \rightarrow \pi^*$  excited states. These variations of the SA scheme, for which no distinct rules exist, uncovered that the influence of these choices onto the excitation energies is up to 0.2 eV, which is quite significant regarding the small energy gap between the states of interest. However, the relative energies of the lowest triplet states are less affected by the SA scheme.

For the largest CAS(14/11), the excitation energies calculated at the CAS-SCF and NEVPT2 level are very similar for the unproblematic excited states (all but  $n_\pi \rightarrow \pi^*$  and  $\pi' \rightarrow \pi^*$ ). Hence, one may conclude that the primary relaxation effects for these state are well described within the orbitals included in the AS. Already for the CAS(12/10) calculations (data not shown, see supporting information) this is no longer true for any of the excited states, leading to the conclusion that all of the orbitals in the CAS are required.

For the  $n_\pi \rightarrow \pi^*$  and  $\pi' \rightarrow \pi^*$  states CAS-SCF and NEVPT2 excitation energies differ significantly. Hence, for these states an even larger AS would be required. This is, however, not feasible since an even larger AS would lead to prohibitively expensive calculations. As soon as perturbation theory is applied to the CAS-SCF(14/11) calculation via the NEVPT2 approach (CAS-NEVPT2), one yields very reasonable agreement with the other high-level calculations for nearly all excited states. Once more, solely the description of the  $S(n_\pi \rightarrow \pi^*)$  is poor and gets even worse from CAS-SCF to NEVPT2 (see figure 4).

Regarding the lowest triplet states, the energy difference predicted at the CAS-NEVPT2 level of theory with the largest AS is only 0.18 eV, which is the second-lowest difference after MOM-CCSD(T) (see below).

Furthermore, the CAS calculations can reveal the multi-reference character of the ground state, which is a critical quantity for accuracy and reliability of all single-reference methods. Using CAS(14/11) with the B2-PLYP geometry, the ground state is dominated by a single reference with a contribution of 81 %. The next larger contribution is that of the doubly excited  $(n_\pi \rightarrow \pi^*)^2$  determinant with 5 %. All other contributions are below 2 %. For the problematic  $n_\pi \rightarrow \pi^*$  excited singlet state on the other hand, the largest determinant has a contribution of only 23 % followed by four similar contributions of 19 %, 18 %, 12 % and 10 %, explaining the problems concerning its theoretical description. The corresponding  $T(n_\pi \rightarrow \pi^*)$  state, however, mainly consists of a singly excited determinant contributing 85 % with only one other small admixture from a triply excited determinant with 2.5 %, which may explain for the large difference between CCSD and CCSD(T) levels of theory. All singlet and triplet  $n \rightarrow \pi^*$  and  $n' \rightarrow \pi^*$  excited states show the same pattern of one big and one small contribution. The bigger one making up

for about 70-75 % of the wavefunction and the smaller one 10-15 %, while any other contributions are 2 % or less.

### Maximum-overlap method

In principle, the MOM-approach allows for a balanced description of the excited states, independent of their character. For this purpose, the SCF is tweaked to converge on the excited state by manipulation of the guess orbitals and application of the MOM-algorithm.<sup>20</sup> Unfortunately, this only works for states, which have no or very little overlap between the involved orbitals, since otherwise the SCF converges back to the ground state. Thus, the MOM approach is not applicable to excited states with large transition moments, which are usually those for which experimental data is available. Hence, the excitation energy of the  $S(\pi' \rightarrow \pi^*)$  state of NB could not be obtained since the SCF calculation falls back to the ground state within the first few iterations. In general, the orbitals resulting from the MOM-SCF are optimized for the respective state, which in combination with high-level CCSD(T) correlation treatment applied here yields very accurate energies of the excited states. Since each state is calculated separately within the MOM approach, this method does not allow for a straightforward calculation of transition moments or any other property involving two or more states.

There are two general drawbacks that may reduce accuracy and reliability of the MOM-approach: At first, the formally incorrect description of the open shell singlet state and secondly, spin contamination of the unrestricted Hatree-Fock (UHF) reference.

A formally correct open-shell singlet wavefunction is a linear combination of two determinants. Within the MOM-approach, however, only one determinant is used that constitutes a 50:50 mixture of the singlet and triplet ( $m_s = 0$ ) eigenfunctions. Consequently, the  $S^2$  expectation value for this single open-shell determinant is 1.0, whereas a formally correct open-shell singlet state has an expectation value of 0.0. For triplet states with  $m_s = \{-1, 1\}$ , for which a single reference is sufficient, the  $S^2$  expectation value is 2.0.

For both, singlet and triplet states an UHF calculation is required to obtain the spin-contaminated open-shell reference wavefunction. At the MOM-CCSD(T) level of theory this problem is compensated by the coupled cluster correlation treatment, which corrects the spin-contamination of the reference wavefunction to some extent for most of the states. This becomes obvious from a comparison of the  $\langle S^2 \rangle$  values for the UHF reference and CCSD wavefunction, which are:  $S(n \rightarrow \pi^*)$  1.59, 0.94;  $T(n \rightarrow \pi^*)$  2.60, 1.94;  $S(n_\pi \rightarrow \pi^*)$  1.52, 0.23,  $T(n_\pi \rightarrow \pi^*)$  2.51, 1.91;  $S(\pi \rightarrow \pi^*)$  1.14, 0.82;  $T(\pi \rightarrow \pi^*)$  2.04, 2.02;  $T(\pi' \rightarrow \pi^*)$ : 2.33, 1.98, respectively.

Furthermore, the issue of CCSD in combination with spin-contaminated UHF references has previously been investigated.<sup>21</sup> The study reports negligible deviations between the CCSD energies for the doublet state of e.g. the  $\text{NO}_2$  molecule calculated with strongly spin-contaminated UHF and spin-pure ROHF references. Nevertheless, the results may be less accurate and less reliable than one would expect from a CCSD(T) calculation for a well-behaved reference.

Besides these theoretical considerations, we may judge the accuracy and reliability of the MOM-approach from a

pragmatic point of view, i.e. by comparison with experimental values and/or the ADC3 results. Indeed, ADC3 and the MOM-approach show remarkable agreement, even for those states exhibiting large spin contamination ( $dE < 0.1$  eV for  $S(n \rightarrow \pi^*)$  and  $S(n' \rightarrow \pi^*)$ ). Hence, we conclude that the MOM-approach can be considered to be very accurate.

The difference between the MOM-CCSD and MOM-CCSD(T) calculations, i.e. the magnitude of the triples-correction may serve as a diagnostic for the importance of correlation effects for each individual excited state. Not surprisingly, the triples correction is more than two times larger for the  $S(n_\pi \rightarrow \pi^*)$  (-0.31 eV) and  $T(n_\pi \rightarrow \pi^*)$  (+0.33 eV) excited states than for any other state. The next largest correction is found for the  $S(\pi \rightarrow \pi^*)$  state, which amounts to 0.16 eV, while it is  $< 0.1$  eV for any other state.

The most surprising result of the MOM-CCSD(T) calculations is the energy of the  $S(n_\pi \rightarrow \pi^*)$  excited-state of 4.4 eV, which is almost 2 eV lower than EOM-CCSD and 1 eV below the ADC3 and DFT/MRCI results (see figure 4). This huge difference is most likely due to the poor description of doubly excited states at the EOM-CCSD level of theory, which is improved at the ADC3 level. Due to the conceptual differences in the MOM-approach, which involves orbital optimization for each state, doubly-excited states are treated with the same accuracy as any other excited state and the ground state.

Combining the energy of MOM-CCSD(T) with the *fosc* predicted by ADC3 (0.037) and EOM-CCSD (0.026), the  $S(n_\pi \rightarrow \pi^*)$  state should be visible in the absorption spectrum. In fact, the gas-phase spectrum of NB published by Nagakura et al. shows a peak with vibrational fine-structure that is found exactly at the predicted energy of 4.42 eV (280 nm).<sup>8</sup> By comparison to unsubstituted benzene, Nagakura et al. attributed this peak to the  $S(\pi \rightarrow \pi^*)$  transition. They corroborate their suggestion with the vibrational progression of the peak which was determined to be 860 /cm in NB compared to 930 /cm in benzene. However, the  $S(\pi \rightarrow \pi^*)$  state has virtually no *fosc* in NB (0.0002 at the ADC3 and 0.007 at the EOM-CCSD levels of theory) and furthermore a significantly higher energy of ~4.7 eV according to ADC3 and MOM-CCSD(T) and 5 eV according to EOM-CCSD. Also the  $S(n' \rightarrow \pi^*)$  state, whose energy of 4.45 eV would be suitable, has negligible *fosc* according to ADC3 (0.0002) and EOM-CCSD (0.0003) that does not increase along any of the molecular coordinates investigated in section 5.

The measured vibrational splitting is identical to the frequency of the ONO bending mode (868 /cm at CCSD/SVP level, 864 /cm at B2-PLYP/def2-TZVP level) along which the  $S(n_\pi \rightarrow \pi^*)$  state exhibits the largest nuclear gradient at the Franck-Condon point of the ground state. Summarizing these results and hints, we suggest that this weak absorption at 4.4 eV in the vapor spectrum of NB is due to the  $S(n_\pi \rightarrow \pi^*)$  excited-state and not the  $S(\pi \rightarrow \pi^*)$  state and, consequently, that the second excited singlet state of NB is a predominantly doubly excited state.

Turning to the energy of the lowest triplet states of NB, MOM-CCSD and MOM-CCSD(T) yield the same state ordering as ADC3, but the energetic gap between  $T(n_\pi \rightarrow \pi^*)$

and  $T(n \rightarrow \pi^*)$  states is much smaller for MOM-CCSD (0.35 eV) and MOM-CCSD(T) (0.14 eV) than for ADC3 (0.52 eV). Since the MOM-CCSD(T) result is presumably the most accurate one, the difference of the vertical energies of the lowest triplet states is in the order of 0.1-0.2 eV. Hence, structural relaxation of the excited states has to be taken into account to answer the question for the globally lowest triplet state. In any case, the  $n \rightarrow \pi^*$  and  $n_\pi \rightarrow \pi^*$  triplet states are most likely closer in energy than predicted at the ADC3 level of theory.

### Structural relaxation in the excited state

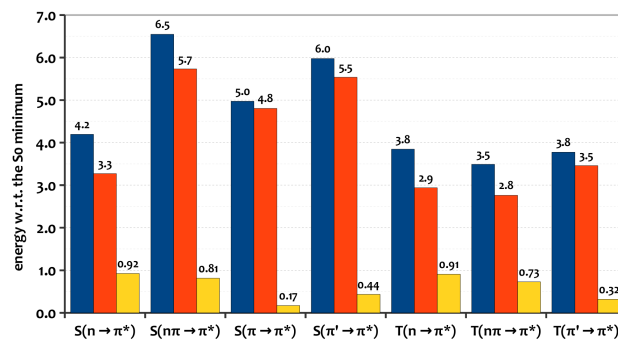


**Figure 5:** Vertical excitation energies (blue), energies of the equilibrium structures of excited states (red) and differences thereof (yellow) relative to the ground-state minimum of nitrobenzene at the EOM-CCSD/cc-pVDZ level of theory in  $C_{2v}$  symmetry. In general, the benefit of structural relaxation is larger for  $n \rightarrow \pi^*$  excited states than for  $\pi \rightarrow \pi^*$  excited states. The  $T(n \rightarrow \pi^*)$  state exhibits a slightly larger relaxation than the  $T(n_\pi \rightarrow \pi^*)$  excited state, reducing the energy difference between these states compared to the vertical excitation energies.

To account for nuclear relaxation, the geometries of all relevant excited states were optimized at the EOM-CCSD level of theory in  $C_{2v}$  symmetry using the cc-pVDZ basis sets. Subsequently, the geometries of the lowest singlet and two lowest triplet states were asymmetrically distorted and then reoptimized without molecular symmetry using the smaller SVP basis set to check whether the states have minima of lower symmetry. Only the  $n_\pi \rightarrow \pi^*$  state has a  $C_s$  symmetric minimum with the oxygen atoms bent out of the molecular plane exhibiting an ONCO out-of-plane angle of  $40^\circ$ . This distortion, however, hardly affects the energy of the relaxed structure ( $dE < 0.03$  eV), as can be seen in the relaxed scan along this ONCO out-of-plane coordinate (see figure 8). Vertical excitation energies and energies of the equilibrium structures of the excited states obtained at the EOM-CCSD/cc-pVDZ level of theory are summarized in figure 5.

In general, geometric relaxation is more pronounced for the  $n \rightarrow \pi^*$  excited states of NB than for the  $\pi \rightarrow \pi^*$  excited states. Focusing on the triplet states, the  $n \rightarrow \pi^*$  excited state shows a slightly larger relaxation contribution than the  $n_\pi \rightarrow \pi^*$  state (0.91 eV vs 0.73 eV). Combining these EOM-CCSD/cc-pVDZ relaxation energies with the MOM-CCSD(T) vertical excitation energies, these lowest triplet states are virtually degenerate. Taking into account the vertical excitation energies obtained with CAS-SCF/NEVPT2,

DFT/MRCI, ADC3, EOM-CCSD or TD-B2-PLYP, which all give the same state ordering as MOM-CCSD(T) but with a significantly larger energy gap, the  $T(n_{\pi} \rightarrow \pi^*)$  state is obtained as the lowest triplet state with an energy gap to the minimum of the  $T(n \rightarrow \pi^*)$  state in the order of -0.05 eV (switched ordering) to 0.5 eV. After all, the ordering of the lowest triplet state of NB in vacuum can not be determined conclusively. However, the  $T(n \rightarrow \pi^*)$  and  $T(n_{\pi} \rightarrow \pi^*)$  states are most likely very close in energy. For the investigation of non-radiative relaxation of NB, it is sufficient to know that these lowest states are almost degenerate. In such a case, the actual ordering is of minor relevance since there is a conical intersection connecting the minima of the two states (see table 1).

Considering the fact that, as will be demonstrated below, the triplet manifold of NB is most likely accessed via ISC from the  $S(n \rightarrow \pi^*)$  to the  $T(n_{\pi} \rightarrow \pi^*)$  state, it is suggestive that the triplet population will end up in the  $T(n_{\pi} \rightarrow \pi^*)$  minimum. From there, thermal population of the  $T(n \rightarrow \pi^*)$  state may be possible, depending on the actual energy gap and the thermal energy available. However, to address such delicate dynamic questions conclusively, advanced quantum-dynamical simulations on highly accurate PES are required. These are, due to the timescale of several hundreds of picoseconds, still out of reach even on most modern computers.

At this point it may thus help to consider the experimentally observed reactivity of nitro-aromats: On the one hand, it has been found that the nitro group can undergo intermolecular and intramolecular hydrogen-abstraction, e.g. in ortho-nitrotoluene, which is only possible in the  $n \rightarrow \pi^*$  excited triplet but not in the  $n_{\pi} \rightarrow \pi^*$  excited triplet state.<sup>10</sup> On the other hand, this reaction reduces the lifetime of the ortho-isomer of nitrotoluene (690 ps) only marginally compared to NB (770 ps).<sup>7</sup> Therefore, one may conclude that the  $n \rightarrow \pi^*$  state has to be thermally accessible from the minimum of the  $n_{\pi} \rightarrow \pi^*$  state at room temperature, but also that either a significant energy gap or a barrier for hydrogen-transfer has to exist since otherwise, the triplet lifetime of ortho-nitrotoluene should be much lower than the one of NB. In an earlier work, this hydrogen transfer has been investigated in ortho-nitrobenzyl acetate (oNBA) at various levels of theory and a substantial barrier of about 0.4-0.5 eV was found.<sup>10</sup> This suggests a rather small splitting of the lowest triplets, since otherwise the hydrogen transfer, for which the energy difference to the  $T(n \rightarrow \pi^*)$  state and the barrier in this state have to be overcome, would presumably not take place at all. To finally answer this question, it will help to determine the temperature-dependent lifetimes of the three isomers of nitrotoluene experimentally and calculate the resulting barrier via an Arrhenius ansatz.

#### Technical details

##### Software

Calculations employing configuration-interaction singles (CIS), CIS with the iterative doubles correction CIS(D), coupled cluster singles, doubles and perturbative triples (CCSD(T)), equation of motion (EOM)-CCSD, maximum-overlap method (MOM)<sup>20</sup> and the algebraic-diagrammatic

construction of second (ADC2) and third order (ADC3)<sup>22,23</sup> were carried out using a development version of the Q-Chem 4.1 program package.<sup>24</sup> The complete active-space self-consistent field (CAS-SCF), *n*-electron valence-state perturbation theory (NEVPT2), B3-LYP and B2-PLYP calculations were conducted using the ORCA 2.9.1 program package.<sup>25</sup> Perturbative coupled-cluster of second order (CC2) and its linear-response variant (LR-CC2) calculations were done with the TURBOMOLE 6.3.1. software.<sup>26</sup> Density-functional theory/multi-reference configuration interaction (DFT/MRCI) and spin-orbit coupling calculations were done with the DFT/MRCI and SPOCK programs, respectively.<sup>27,28,29,30</sup>

##### Basis sets

For all energy calculations along the NO stretching, ONO bending and ONCO out-of-plane coordinates the def2-TZVP(-f) basis set was employed,<sup>31</sup> which is obtained from the standard def2-TZVP basis set by deleting the computationally most expensive f-type polarization functions. For the ADC3 calculations, this modification significantly reduces computational cost while it hardly affects the results ( $dE < 0.05$  eV). Calculations of the vertical excitation energies at the ground state equilibrium geometry were carried out with the unmodified def2-TZVP basis set. The MOM-CCSD(T) single-point energy calculation for the  $S(n_{\pi} \rightarrow \pi^*)$ ,  $T(n_{\pi} \rightarrow \pi^*)$  and  $T(n \rightarrow \pi^*)$  states was carried out with the def2-TZVP(-f) and cc-pVTZ<sup>32</sup> basis sets, since we were unable to converge the unrestricted SCF reference in the calculation with def2-TZVP. The results of these calculations are lying within 0.02 eV for excitation energies and excitation energy differences. For the calculation of the  $S(n \rightarrow \pi^*)$ ,  $T(n \rightarrow \pi^*)$  and  $T(n_{\pi} \rightarrow \pi^*)$  relaxed potential energy surface cuts along ONO bending and ONCO out-of-plane modes at EOM-CCSD level of theory, the basis set quality was reduced to def2-SVP to reduce the computational effort.<sup>31</sup>

##### Symmetry

All calculations were carried out exploiting  $C_{2v}$  symmetry of the NB molecule. Only along the ONCO out-of-plane coordinate and for some of the excited state optimizations the symmetry was reduced to  $C_s$  and  $C_1$  as mentioned in the text.

##### Traceability

In an attempt to make this work as reproducible and traceable as possible, all input and output files have been made available in the supporting information. Hence, all calculations and results can easily be repeated and extended, given that software (Q-Chem 4.1, ORCA 2.9.1, and TURBOMOLE 6.3.1.) and sufficient computational resources (~200 GB RAM for MOM-CCSD(T), EOM-CCSD and ADC3 with the def2-TZVP basis) are present. The only exception are the ADC3 and DFT/MRCI calculations, for which a development versions of the respective software has been used. A publication on the implementation of ADC3 is in preparation and the code will be released along with one of the next versions of Q-Chem.

## 5) Mechanism of non-radiative relaxation

### Approach

By comparison of the ground- and excited-state equilibrium structures (see table 1) we identified the coordinates that will presumably be relevant for the non-radiative relaxation processes. The four coordinates that exhibit the largest changes between ground and excited state geometries of the lowest excited states are the NO and CN bond lengths as well as ONO-angle and the ONCO out-of-plane improper dihedral (given as the displacement from the planar structure: ONCO out-of-plane =  $180 - (\text{ONCO dihedral})$ ). Out of these coordinates, only the latter has been previously inferred to be relevant for NB photochemistry and investigated by Takezaki and Quenneville et al. (for a summary of the existing literature see section 2).<sup>13</sup>

To obtain a coarse overview, rigid scans were carried out using the ground state equilibrium structure as a starting point and ADC3/SVP single-point calculations to yield ground- and excited-state energies (see supporting information). It was found that along the CN bond length as well as along the nitro group tilting (CCNO dihedral) coordinates the PES of ground and excited states are almost flat and virtually parallel, so that crossings between these states are absent. Therefore, these coordinates were excluded from further investigations.

Along the unrelaxed ONO bending, ONCO out-of-plane and NO stretching coordinates, on the contrary, numerous crossings between all relevant states exist. To improve the theoretical description, the scans along the ONO bending and ONCO out-of-plane coordinates were refined. For this purpose, the unrelaxed structures of the preliminary calculations were optimized at the EOM-CCSD/SVP level of theory to obtain relaxed PES of the relevant states and coordinates. Along these relaxed scans, ADC3/def2-TZVP(-f) as well as DFT/MRCI/def2-TZVP single point calculations were carried out to obtain energies and spin-orbit coupling (SOC) elements for the relevant excited states.

In the following, only the energies obtained with ADC3 are shown and discussed, which is due to their much better agreement with experimental results and high-level calculations compared to DFT/MRCI (see section 4 and figure 5 for details). For the latter, the excitation energies are too low compared to experimental values and high-level calculations, which is true in particular for the  $S(n \rightarrow \pi^*)$  excited state ( $S_1$ ). As a result from this erroneous description, one would expect ultrafast deactivation via the artificially lowered  $S_1/S_0$  CI (almost 1 eV below the  $S_1$  at the FC-point) along the ONO bending and hardly any population of the triplet state via ISC. Since this is obviously not the case, we will omit the PES calculated with DFT/MRCI in the discussion. The spin-orbit-coupling elements calculated with DFT/MRCI, however, show very good agreement with those obtained with CAS-NEVPT2 for the ground state equilibrium geometry.

The energies for the key points of the PES (crossing points, conical intersections and excited state minima) given in the text below have been obtained at EOM-CCSD/cc-pVDZ level of theory since this method allows for minimum energy crossing point (MECP) optimizations. These energies and geometric parameters for these point are summarized in table 1. For the respective values estimated from the ADC3/def2-TZVP(-f) PES, see figure 9.

**Table 1:** Relative energies and structural parameters for the most relevant points of the potential energy surface of nitrobenzene at the (EOM-)CCSD/cc-pVDZ level of theory. Energies for each of the relevant points on the PES are given with respect to the next accessible minimum as well as  $S_1$  and ground state ( $S_0$ ) energies at the Franck-Condon point. In this table, for the sake of compactness  $T_1$  is used to abbreviate the  $T(n_\pi \rightarrow \pi^*)$  state and  $T_2$  for the  $T(n \rightarrow \pi^*)$  state.

point on the PES:		energy [eV] with respect to:			relevant bond lengths [ $\text{\AA}$ ] and angles [degree]			
		lowest accessible minimum	$S_1$ at FC point	$S_0$ at FC point (global min.)	r(CN)	r(NO)	(ONO) bending	(ONCO) out-of-plane
$S_0$ minimum	$C_{2v}$	-	-4.20	-	1.483	1.221	125.4	0
$S_1$ minimum	$C_{2v}$	-	-0.92	3.27	1.392	1.293	106.3	0
CI( $S_1/S_0$ )	$C_{2v}$	0.63 ( $S_1$ )	-0.29	3.91	1.357	1.324	88.2	0
CI( $S_1/S_0$ )	$C_s$	0.43 ( $S_1$ )	-0.49	3.71	1.422	1.324	91.1	47.9
X( $S_1/T_1$ )	$C_{2v}$	0.03 ( $S_1$ )	-0.89	3.31	1.383	1.289	102.1	0
$T_1$ minimum	$C_s$	-	-1.44	2.76	1.426	1.307	115.9	38.0
$T_2$ minimum	$C_{2v}$	0.18 ( $T_1$ )	-1.26	2.94	1.398	1.292	106.2	0
X( $T_1/S_0$ )	$C_s$	0.22 ( $T_1$ )	-1.21	2.98	1.449	1.327	97.1	54.0
CI( $T_1/T_2$ )	$C_{2v}$	0.19 ( $T_1$ )	-1.25	2.95	1.404	1.300	108.8	0

### Initial internal-conversion to $S_1$

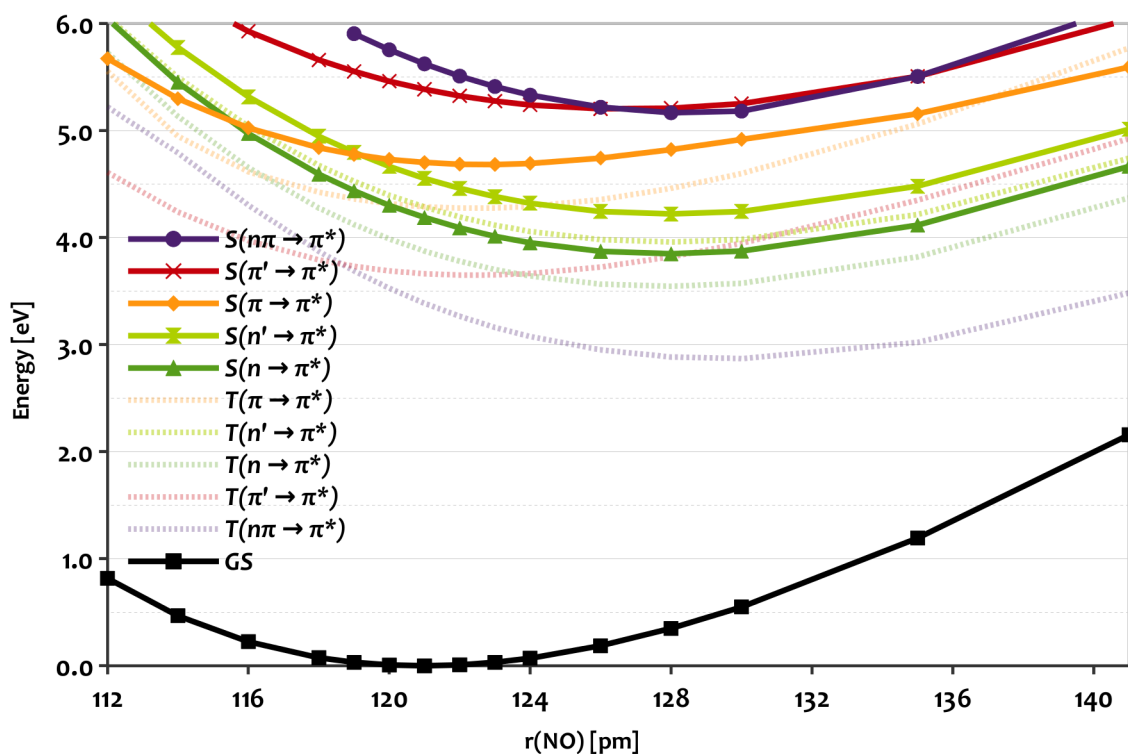


**Figure 6:** Unrelaxed potential energy surfaces along the symmetric NO-stretching mode at the ADC3/def2-TZVP(-f) level of theory. Singlet states are depicted as continuous lines, triplet states as transparent, dashed lines. Corresponding singlet and triplet states have the same color

Lets first turn to the theoretical investigation of the fastest, experimentally observed process, for which an upper limit of 100 fs has been reported.<sup>14</sup>

For an excitation of the bright  $S(\pi' \rightarrow \pi^*)$  state, one may speculate that this process could be IC to  $S_1$  since there is a continuous path from the bright state to the lowest singlet state (figure 6). This complete path is lying below the energy

of the bright state at the FC point. Hence, if energy conservation is assumed, IC from the bright  $S(\pi' \rightarrow \pi^*)$  to  $S_1$  should be possible in the given time window that equals a few vibrational periods of the symmetric NO stretching mode. In this case, a large fraction of the initial excitation energy that is released during IC from the bright state to  $S_1$  will end up in this symmetric NO stretching mode.

In their experiments, however, Takezaki et al. directly excited the  $S_1$  state at 280 nm (see figure 9) and there has to be another process causing this ultrafast component. For cooling of the  $S_1$  population, as inferred by Takezaki et al., this process is at least an order of magnitude too fast. In similar aromatic molecules, internal vibrational equilibration (IVR) and cooling take place on timescales of 1 and 10 ps, respectively.<sup>33</sup> We think this ultrafast signal is caused by IC of a fraction (about 20 % under go IC instead of ISC) of the vibrationally excited  $S_1$  population to the ground state via the  $S_1/S_0$  CI along the ONO bending coordinate (figure 7, see below)

#### First inter-system crossing (ISC) into the triplet manifold and IC to the ground state

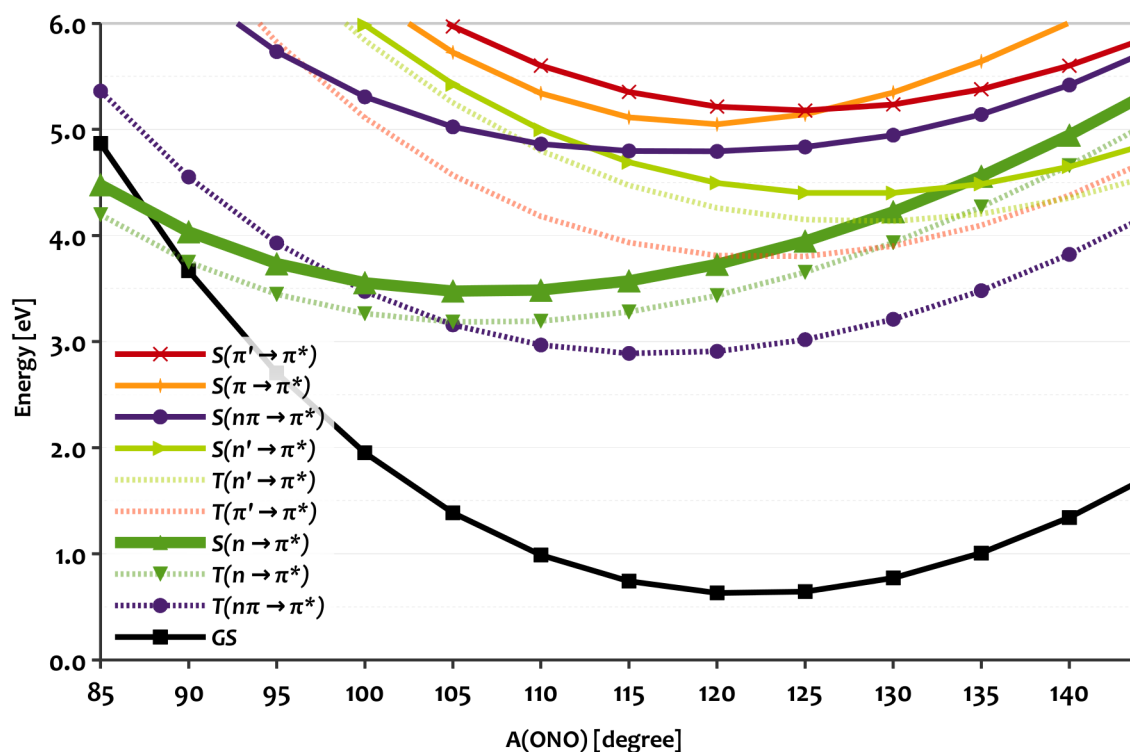


**Figure 7:**  $S(n \rightarrow \pi^*)$  relaxed (thick green line) surface of the ONO-bending coordinate at the ADC3/def2-TZVP(-f)/EOM-CCSD/SVP level of theory. Right next to its minimum, the  $S(n \rightarrow \pi^*)$  state crosses the  $T(n_\pi \rightarrow \pi^*)$  state, which together with the large spin-orbit coupling between those two states explains the fast and efficient inter-system crossing. At even larger distortions and higher energy the  $S(n \rightarrow \pi^*)$  state also crosses the  $S_0$ , which most likely is the channel for the observed 20 % of the population that do not undergo ISC but IC.

Eventually, the population has reached  $S_1$  either via IC or directly via excitation of the weak  $S(n \rightarrow \pi^*)$  band, like in the experimental investigations described in section 2. For the ISC into the triplet manifold with a quantum yield of 80 %, a timescale of 6 ps has been reported, whereas the other 20 % undergo IC back to the ground state. After 6 ps, it can be assumed that IVR and cooling of the population in  $S_1$  is largely progressed. Hence, to explain for ISC on such a timescale, one would expect an energetically accessible crossing between the  $S(n \rightarrow \pi^*)$  and  $T(n_\pi \rightarrow \pi^*)$  states in close proximity to the  $S(n \rightarrow \pi^*)$  minimum exhibiting large SOC. Furthermore, a CI between the  $S(n \rightarrow \pi^*)$  and the

ground state should be present that is energetically and structurally further away but yet accessible immediately after the excitation to explain for the remaining 20 % of the population that do not undergo ISC but instead IC.

This is exactly what is found for the  $S_1$  optimized PES shown in figure 7. The crossing between  $S_1/T(n_\pi \rightarrow \pi^*)$  is found to be virtually degenerate with the  $S_1$  minimum ( $\Delta E < 0.03$  eV), while the  $S_1/S_0$  CI is significantly higher in energy ( $\Delta E = 0.63$  eV) but still below the energy of the  $S_1$  at the FC point (FC point: 4.2 eV,  $S_1$  minimum: 3.3 eV, see table 1 for all the data).

Accordingly, we suggest the following mechanistic picture:

Due to the gradient in the  $S_1$  state at the FC point, the population will reach the  $S_1$  minimum with a momentum pointing in the direction of the crossings with the  $T(n_\pi \rightarrow \pi^*)$  and the ground state. Regarding the initial excitation energy of the  $S_1$  state at the FC point, which is only slightly below to the energy of the  $S_1/S_0$  CI, we assume that only immediately after the initial excitation IC to the ground state is possible via this CI. Already about 100 fs later, too much energy may be dissipated via IVR and cooling, effectively trapping the population in the  $S_1$  minimum. From there, only the crossing point with the  $T(n_\pi \rightarrow \pi^*)$  state is accessible. At this crossing point, the SOC calculated at the DFT/MRCI level of theory is about 50 /cm, which causes the remaining population in  $S_1$  to undergo ISC into the triplet-manifold.

To verify our hypothesis, we suggest the following experiment, in which the excitation energy of NB is to be varied (e.g. by excitation of the bright  $S(\pi' \rightarrow \pi^*)$  state instead of the  $S(n \rightarrow \pi^*)$  state) while the quantum yield of the population undergoing either IC or ISC is to be measured. The outcome should be different depending which UV-band of NB is initially excited. This is due to the fact that the vibrational excess energy available for the molecules immediately after the excitation discriminates between IC and ISC or in other words the  $S_1/S_0$  and  $S_1/T(n \rightarrow \pi^*)$  state crossings. To allow for more quantitative predictions of the outcome of these experiments, quantum-dynamics simulations should be performed.

Besides  $S_1/S_0$  IC along the ONO bending coordinate, there is in principle another possibility for this IC along the ONCO out-of-plane coordinate as can be seen in figure 8. Although the latter is optimized for  $T(n_\pi \rightarrow \pi^*)$ , the  $S_1$  optimized surface is very similar. A  $S_1/S_0$  IC along this CI involving the out-of-plane bending has been suggested by Quenneville et al.. According to EOM-CCSD/cc-pVDZ the position of this CI is 0.43 eV above the  $S_1$  minimum, which is 0.2 eV lower than the  $C_{2v}$  symmetric CI along the ONO bending coordinate (see table 1). Nevertheless, we do not expect the IC along the ONCO coordinate to be of major relevance for two reasons. At first, the out-of-plane bending is not FC active as it experiences no gradient in any of the singlet excited states (the relaxed excited-state structures are all planar). Secondly, this out-of-plane bending is only weakly coupled to the FC active modes, since the latter are all in-plane modes. The ONO bending mode, on the contrary, is one of the two FC active coordinates exhibiting the largest gradient on the  $S_1$  surface at the FC point (see figure 7). Hence, immediately after excitation and IC to the  $S_1$  mainly the ONO bending and NO stretching modes may be vibrationally excited and the primary internal-vibrational redistribution (IVR) does most likely not include the ONCO out-of-plane mode. Only via interaction with the solvent and indirect IVR, the ONCO out-of-plane mode may receive a fraction of the vibrational energy. After all, any process taking place mainly along the ONCO coordinate that involves crossing a barrier of 0.4 eV will presumably be much slower compared to a similar process along the ONO coordinate, although the barrier there is 0.6 eV.

### Second ISC to the ground state

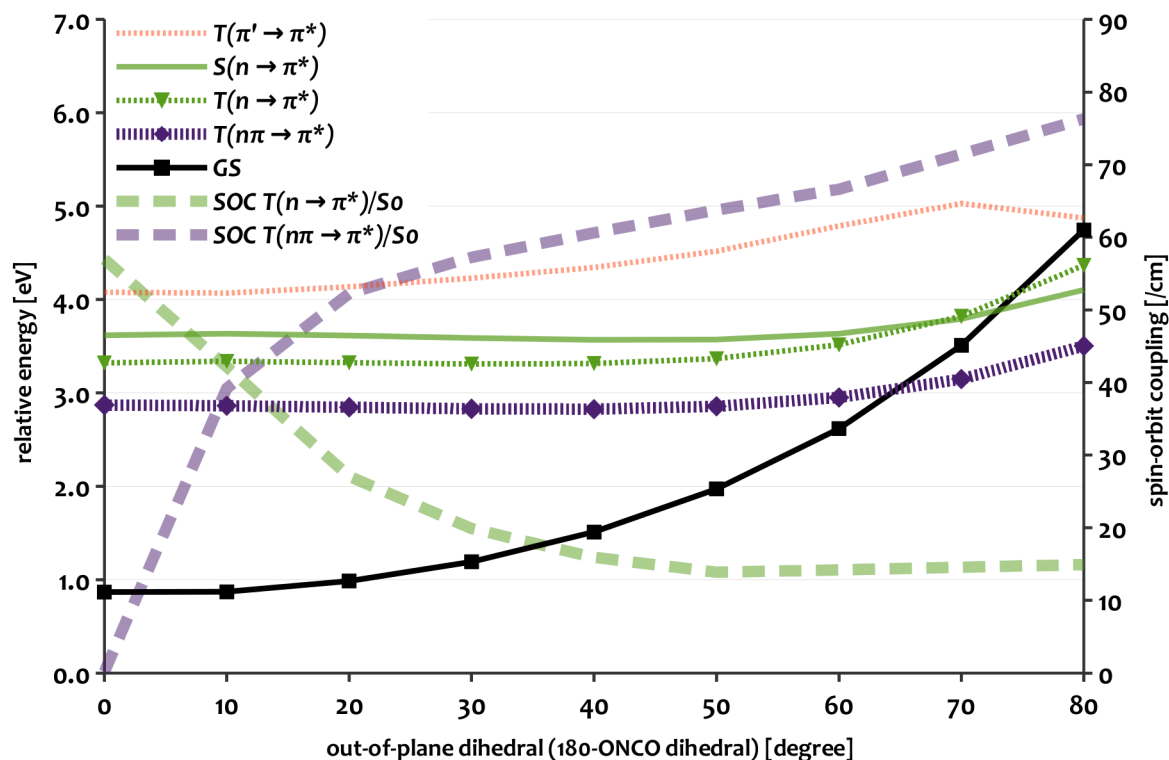


**Figure 8:**  $T(n_{\pi} \rightarrow \pi^*)$  relaxed potential energy surface of the ONCO dihedral angle at the ADC3/def2-TZVP(-f)/EOM-CCSD/SVP level of theory in  $C_s$  symmetry. Additionally, the spin-orbit coupling elements (SOC) between the lowest triplets and the ground-state (bold, transparent lines) obtained at DFT/MRCI level of theory are shown on a secondary y-axis (right).

After all, 80 % of the population end up in the  $T(n_{\pi} \rightarrow \pi^*)$  state, from which the ground state is regenerated via ISC within hundreds of picoseconds depending on solvent and temperature.<sup>5</sup> To investigate this second ISC back to the ground state, the  $T(n_{\pi} \rightarrow \pi^*)$  optimized ONO bending and ONCO out-of-plane coordinates were calculated. For this second ISC process, one condition has changed compared to initial IC and ISC processes. When reaching the triplet manifold on a timescale of 6 ps, the NB molecules will presumably be completely equilibrated internally as well as with the environment and consequently, the energy available will be equal or at least very close to the thermal energy. Hence, this second ISC should be seen as a classical thermo-chemical reaction which is corroborated by the temperature dependent rate constant reported by Takezaki et al..

Regarding the  $T(n \rightarrow \pi^*)$  optimized PES along the ONCO coordinate (figure 8), a thermal excitation to  $T(n_{\pi} \rightarrow \pi^*)$  via the crossing along the ONO bending coordinate can be excluded at room temperature due to the large energy difference of about 0.5 eV between these states, at least at the ADC3 level of theory. Remembering the results from section 3 and 4, which hint towards a much smaller energy gap as predicted by ADC3, the  $T(n \rightarrow \pi^*)$  state may be thermally accessible after all.

The actual energy gap and the state ordering are, however, irrelevant concerning the validity of our hypothesis. Along the ONCO out-of-plane mode, both lowest triplet states exhibit an energetically accessible crossing with the ground state at an

ONCO out-of-plane angle of  $\sim 65^\circ$  and  $70^\circ$ , respectively. For both states the barrier towards the CI with the ground state is approximately the same. Hence, even if the lowest triplet states are energetically degenerate, the pathway for non-radiative relaxation is determined rather by the magnitude of SOC with the ground state.

Although the SOC between the  $T(n_{\pi} \rightarrow \pi^*)$  state and the ground state is zero according to El-Sayed's rules and our calculations for the  $C_{2v}$  symmetric equilibrium geometry, this changes dramatically as soon as the molecule is distorted along this ONCO out-of-plane coordinate. For ONCO out-of-plane bending angles larger than  $10^\circ$  the SOC between ground state and  $T(n_{\pi} \rightarrow \pi^*)$  state is larger than that of the  $T(n \rightarrow \pi^*)$  state (see figure 8). Hence, the second ISC will presumably take place along the ONCO out-of-plane bending in the  $T(n_{\pi} \rightarrow \pi^*)$  state in a classical thermo-chemical reaction and the barrier that has to be overcome is given as the difference between the  $T(n_{\pi} \rightarrow \pi^*)/S_0$  crossing point and the  $T(n_{\pi} \rightarrow \pi^*)$  minimum, which is 0.15 eV at the EOM-CCSD/cc-pVDZ level of theory in  $C_s$  symmetry (see table 1). To eliminate restrictions introduced by symmetry, we calculated the minimum-energy crossing point (MECP) additionally at the B2-PLYP level of theory using ORCA. Starting from the EOM-CCSD/SVP optimized geometry closest to the crossing point in figure 8 (ONCO out-of-plane of  $60^\circ$ ), the MECP optimization was carried out using the closed-shell variant of B2-PLYP for the ground state and the unrestricted open-shell variant for the  $T(n_{\pi} \rightarrow \pi^*)$  state. B2-PLYP was chosen for this

purpose due to its very good agreement with ADC3 for the vertical excitation energy of  $T(n_{\pi} \rightarrow \pi^*)$  (see figure 3), which in combination with its low computational demands enables one to carry out a vibrational analyses at the crossing point and respective minimum. In perfect agreement with the EOM-CCSD calculations in  $C_s$  symmetry (see table 1), the difference of the total energies between  $T(n_{\pi} \rightarrow \pi^*)$  minimum and the MECP between  $T(n_{\pi} \rightarrow \pi^*)$  and the ground state is 0.15 eV. Furthermore, it was found that this value is hardly affected by thermal and entropical corrections (+0.01 eV).

Using the temperature-dependent lifetimes of the triplet state reported by Takezaki et al. to calculate the energy barrier of this reaction via a simple Arrhenius ansatz, one obtains an activation energy of approximately 0.084 eV, which is in very reasonable agreement with our theoretical results (for the calculation see supporting information).

Finally, one may ask why this second ISC process back to the ground state is two orders of magnitude slower than the ISC into the triplet manifold. We think there are three main reasons. At first, the molecule is much colder at the time of the second ISC, which is true in particular for the relevant ONCO out-of-plane coordinate, that is not Frank-Condon active at all. Secondly, the energetic distance of the crossing point to the minimum is much lower for the first ISC than for the second (0.03 eV vs. 0.15 eV) and finally, the ONCO out-of-plane coordinate is a large amplitude motion that deforms the molecule out of its planar structure. Hence, this motion is hindered by solvent molecules, which might provide an explanation for the chain-length dependent rate-constant found by Takezaki et al.. The higher the viscosity of the solvent, the more energy is required for its displacement and hence also for this motion to be carried out.

## 6) Summary & Conclusion

Despite being subject of research for more than 100 years, there are still many open questions regarding the photochemical and photophysical processes as well as the underlying electronic structure of electronically excited nitroaromatic compounds and their parent nitrobenzene (NB). On the experimental side, this was traced back to the non-radiative character of the relaxation processes in NB, while on the theoretical side, the involved electronic structure of NB complicates their computation.

Here, we reported an extensive theoretical investigation with the aim of establishing a reliable and accurate methodology for the description of NB (section 4). Subsequently, potential energy surfaces (PES) of NB were investigated employing high level single- and multi-reference *ab initio* and DFT methods featuring the recently implemented ADC3 and DFT/MRCI (section 5), which allow for an accurate and balanced description of singly and doubly excited states as well as for a calculation of spin-orbit couplings (SOC).

The difficulties with the theoretical description of NB could be traced back to a low-lying singlet state with large double-excitation character of about 50 % at an energy of 4.4 eV according to MOM-CCSD(T). In very good agreement with excitation energy, vibrational splitting and oscillator strength,

this state was assigned to the lowest energy peak in the experimental absorption spectrum of NB vapor. It constitutes the second lowest excited singlet state of NB at the ground state equilibrium geometry.

As a results of its large double excitation character and thus great importance of secondary (electronic) relaxation effects, the calculated vertical excitation energy of this  $B_1 n_{\pi} \rightarrow \pi^*$  excited singlet state ranges from 6.3 eV (EOM-CCSD) to 4.4 eV (MOM-CCSD(T)), with ADC3 (5.4 eV) and DFT/MRCI (5.2 eV) in between. The difficulties in its theoretical description and the resulting inaccuracy persist for the corresponding  $1^3B_1$  triplet state. As a consequence, the riddle of the character of the lowest triplet state of NB, for which the  $1^3A_2 T(n \rightarrow \pi^*)$  and  $1^3B_1 T(n_{\pi} \rightarrow \pi^*)$  states are good candidates, could not be ultimately resolved. Concluding the results of the highest level single- and multi-reference calculations, it seems that the  $T(n_{\pi} \rightarrow \pi^*)$  is slightly below the  $T(n \rightarrow \pi^*)$  state at the Franck-Condon (FC) point ( $\Delta E$  MOM-CCSD(T): 0.14 eV, CAS-NEVPT2(14/11): 0.18 eV). Including nuclear relaxation effects obtained at the EOM-CCSD level of theory, which favor the  $T(n \rightarrow \pi^*)$  state a little bit more (-0.92 eV vs. -0.73 eV), the small energy difference is decreased even further, yielding two virtually degenerate triplet states. According to ADC3, however, the difference is significantly larger at the Franck-Condon geometry (0.52 eV) and prevails when relaxation effects are included.

At this point, it is unclear whether ADC3 or MOM-CCSD(T) and CAS-NEVPT2 yield more accurate results. There are valid arguments for and against all of these methods. Although MOM-CCSD(T) should in general be more accurate than ADC3, it suffers from serious spin contamination of the reference and there exists not much experience on how this may affect the accuracy of the method. For any other than the  $n_{\pi} \rightarrow \pi^*$  excited states of NB, however, MOM-CCSD(T) shows very good agreement with experimental values and other high level calculations despite spin-contamination. For the CAS-NEVPT2 calculations, tweaking of the state-averaging (e.g. equal weights for each class of states, equal weight for each state, inclusion of further/less states in the averaging scheme etc.) allows one to obtain almost any desired result within 0.1-0.3 eV. Hence, it is left to future studies employing even higher-order methods to determine the character of the lowest triplet state of NB. For the investigation of the non-radiative relaxation pathways of NB, it was sufficient to know the character of the lowest two triplet states and that they are almost degenerate.

To study the non-radiative relaxation processes, the relaxed PES of the relevant states along the symmetric NO stretching, ONO bending and ONCO out-of-plane bending coordinates of the NB molecule. For this purpose we have chosen the ADC3 model for energies and DFT/MRCI to obtain spin-orbit-couplings (SOC).

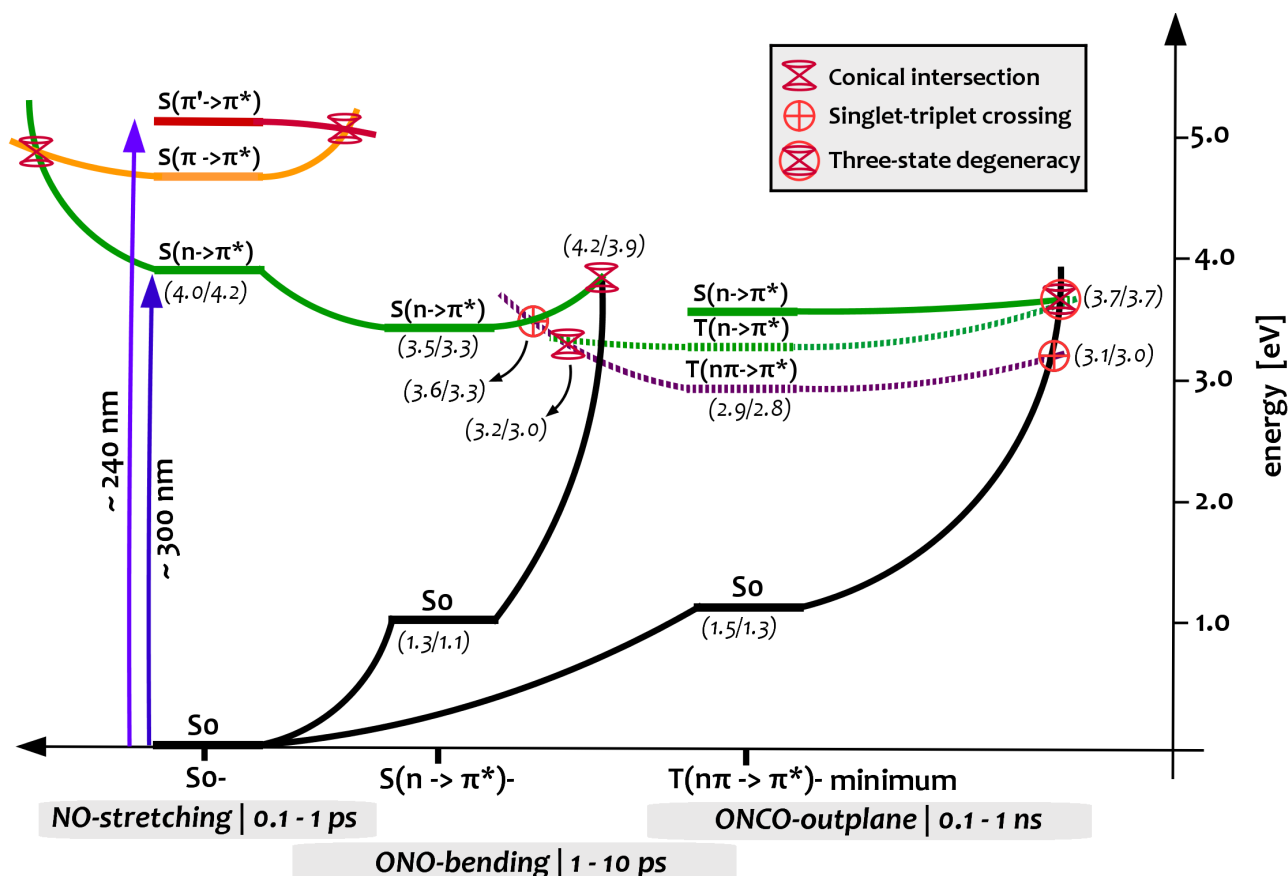


**Figure 9:** Schematic potential-energy surface of the non-radiative relaxation pathways of nitrobenzene based on the ADC3 and EOM-CCSD calculations. This scheme summarizes the relaxed surface scans, relating conical intersections and singlet-triplet crossings to the coordinates and timescales of the non-radiative relaxation processes. ADC3 and EOM-CCSD energies in eV for the key points of the PES are given in parenthesis (ADC3/CCSD).

**The first and fastest decay process** is observed on a timescale  $< 100$  fs in the experimental investigation, in which the  $S_1$  is directly excited. Our results suggest this process to be the internal conversion (IC) of a fraction (about 20 %) of the vibrationally excited  $S_1$  population to the electronic ground-state via an energetically high-lying conical intersection (CI) along the ONO bending coordinate. A few hundreds of femtoseconds later, too much energy is dissipated to reach the CI, effectively trapping the population in  $S_1$ .

If NB is excited into its bright  $S(\pi \rightarrow \pi^*)$  state, IC to  $S_1$  will presumably take place on a similar timescale along the NO stretching coordinate, along which there exists a continuous pathway well below the initial excitation energy. Since there will be much more vibrational excess energy available to the molecules after IC to  $S_1$ , we suggested that in case of excitation of the bright state, the fraction of the population undergoing IC instead of ISC will be significantly larger.

**Inter-system crossing (ISC) from  $S_1$  to the triplet manifold** was reported to occur on a 6 ps timescale exhibiting a quantum yield of 80%. Our calculations show that indeed, the  $T(n_\pi \rightarrow \pi^*)$  state crosses the minimum of the  $S_1$  along the ONO bending mode ( $\Delta E$  0.04 eV, see table 1). For the crossing point, one obtains a SOC in the order of 50 /cm, which explains for the unusually fast and efficient ISC of NB.

**The second ISC from the triple manifold back to the**

**ground state** has been found to occur on a timescale of hundreds of picoseconds, depending on temperature and surprisingly also the chain length of the aliphatic solvent. Due to the much longer timescales of this process, one can expect the molecules to be equilibrated with their environment. Our results corroborate the hypothesis of Takezaki et al., who suggested this final relaxation to occur along the ONCO out-of-plane coordinate. In the  $T(n_\pi \rightarrow \pi^*)$  relaxed PES along this coordinate, there are crossings between both low-lying triplet states with the ground state, for each of which there is significant SOC. Since, however, the SOC at the crossing points is about three times larger between the energetically favored  $T(n_\pi \rightarrow \pi^*)$  state and the ground state than for the  $T(n \rightarrow \pi^*)$  state (75 /cm vs. 15 /cm, see figure 8), we suggested the second ISC to the ground state to occur from the  $T(n_\pi \rightarrow \pi^*)$  state. Due to an almost flat run of the lowest two triplet states along this coordinate, the  $T(n_\pi \rightarrow \pi^*)/S_0$  crossing is found at an energy only 0.15 eV above the relaxed  $T(n_\pi \rightarrow \pi^*)$  minimum. This is in very reasonable agreement with the experimentally observed temperature dependency that translates into a barrier of 0.08 eV according to the Arrhenius formalism.

After all, the non-radiative relaxation of electronically excited NB is explained conclusively and in good agreement with experimental observations. Furthermore, we shed light on the riddle of the nature of the lowest triplet state of NB.

Finally, we want to point out a parallel between the failure of CC2 for NB and the problems concerning the description of ozone, which is isoelectronic to  $\text{NO}_2^-$  and therefore related to the aromatic nitro group. The PES of  $\text{NO}_2^-$  has been investigated and compared to PES obtained with MP2, CCSD and CCSDT by Pabst et al.,<sup>34</sup> who discovered very similar problems leading to the same overestimation of the NO bond-length by CC2 that we reported here. In their work, the problems are traced back to the structure of the CC2 model in combination with significant singlet double-radical character of ozone and  $\text{NO}_2^-$ . They emphasize that CC2 was developed aiming at the description of excited states, but not as an improvement over MP2 for ground state geometries, for which the latter should be preferred. Regarding our results, we want to reface their warning and suggest not to use CC2 for optimization of systems containing an aromatic or aliphatic nitro group.

## Acknowledgment

Funding by the German National Research Council (Deutsche Forschungsgemeinschaft DFG, project MA 1051/12-1) is gratefully acknowledged.

J.-M. Mewes wants to thank Felix Plasser and Peter Gilch for helpful discussions and the Heidelberg Graduate School for Mathematical and Computational Sciences (HGS MathComp) for funding and computer time.

## Notes and references

<sup>a</sup> *Interdisciplinary Center for Scientific Computing, Ruprecht-Karls University, Im Neuenheimer Feld 368, 69120 Heidelberg;*

**E-mail: dreuw@uni-heidelberg.de**

<sup>b</sup> *Institut Theoretische Chemie und Computerchemie, Gebäude 26.32 Raum 03.40 und 03.42, Universitätsstraße 1, 40225 Düsseldorf;*

**E-mail: cm@theochem.uni-duesseldorf.de**

† Electronic Supplementary Information (ESI) available: Available are input and output files for all calculations as well as raw data of the shown plots, figures and tables in open document format.

See DOI: 10.1039/b000000x/

- G. Ciamician, P. Silber, multiple publications in *Berichte der deutschen chemischen Gesellschaft*, 1900-1910, **30-38**; nitro aromats in particular in *Chem. Ber.*, 1901, **34** p. 2040 and 1902, **35**, p. 1992.
- A. P. Pelliccioli, J. Wirz, *Photochem. Photobiol. Sci.*, 2002, **1**, p. 441
- J. Henzl, M. Mehlhorn, K. Morgenstern, *Nanotechnology*, 2007, **18**, p. 495502
- G. C. R. Ellis-Davis, *Nature Methods*, 2007, **4**, p. 619
- M. Takezaki, N. Hirota, M. Terazima, *J. Phys. Chem. A*, 1997, **101**, p. 3443
- R. Hurlley and A. C. Testa, *J. Am. Chem. Soc.*, 1968, **90** p. 1951
- R. W. Yip, D. K. Sharma, R. Giasson, D. Gravel, *J. Phys. Chem.*, 1984, **88**, p. 5770
- S. Nagakura, M. Kojima, Y. Maruyama, *J. Mol. Spec.*, 1964, **13**, p. 174
- K. Schaper, M. Etinski, T. Fleig, *Photochemistry and Photobiology*, 2009, **85**, 1075–1081
- J. Mewes, A. Dreuw, *J. Phys. Chem. A*, 2013, **15**, p. 6691
- A. Dreuw, M. Head-Gordon, *J. Am. Chem. Soc.*, 2004, **126**, p. 4007
- A. Domenicano, G. Schultz, I. Hargittai, M. Colapietro, G. Portalone, P. George, C. W. Bock, *Struct. Chem.*, 1990, **1**, p. 107
- M. Takezaki, N. Hirota, M. Terazima, *J. Phys. Chem. A*, 1998, **108**, p. 4685
- M. Takezaki, N. Hirota, M. Terazima, H. Sato, T. Nakajima, S. Kato, *J. Phys. Chem. A*, 1997, **101**, p. 5190
- J. Quenneville, M. Greenfield, D. S. Moore, S. D. McGrane, R. J. Scharff, *J. Phys. Chem. A*, 2011, **115**, p. 12286
- H. Görner, *Photochem. Photobiol. Sci.*, 2005, **4**, p. 822
- J. Kohl-Landgraf, F. Buhr, D. Lefrancois, J.-M. Mewes, H. Schwalbe, A. Dreuw, J. Wachtveitl, *J. Am. Chem. Soc.*, 2014, **136**, p. 3430
- T. Schmierer, F. Bley, K. Scharper, P. Gilch, *J. Photochem. Photobiol. A*, 2011, **217**, p. 363
- M. A. El-Sayed, *J. Chem. Phys.*, 1963, **38**, p. 2834
- A. T. B. Gilbert, N. A. Besley, P. M. W. Gill, *J. Phys. Chem. A*, 2008, **112**, p. 13164
- J. F. Stanton, *J. Chem. Phys.*, 1994, 101, p. 371
- P. H. P. Harbach, M. Wormit, A. Dreuw, in preparation.
- A. B Trofimov, G. Stelter, J. Schirmer, *J. Chem. Phys.*, 1999, **111**, p. 9982
- A. I. Krylov, P. M. W. Gill, *WIREs Comput. Mol. Sci.*, 2013, **3**, p. 317
- F. Neese, *WIREs Comput. Mol. Sci.*, 2012, **2**, p. 73
- R. Ahlrichs, M. Bär, M. Häser, H. Horn and C. Kölmel, *Chem. Phys. Lett.*, 1989, **162**, p. 165
- S. Grimme, M. Waletzke, *J. Chem. Phys.*, 1999, **111**, p. 5645
- M. Kleinschmidt, C. M. Marian, S. Grimme, M. Waletzke, *J. Chem. Phys.*, 2009, **130**, p. 44708
- M. Kleinschmidt, J. Tatchen, C. M. Marian, *J. Comp. Chem.*, 2003, **23**, p. 824
- M. Kleinschmidt, C. M. Marian, *Chem. Phys.*, 2005, **311**, p. 71
- F. Weigend and R. Ahlrichs, *Phys. Chem. Chem. Phys.* 2005, **7**, p. 3297
- T.H. Dunning Jr., *J. Chem. Phys.*, 1989, **90**, p. 1007
- T. Elsaesser, W. Kaiser, *Annu. Rev. Phys. Chem.*, 1991, **42**, p. 83
- M. Pabst, A. Köhn, J. Gauss, J. F. Stanton, *Chem. Phys. Lett.*, 2010, **495**, p. 135

- [1] G. Ciamician, P. Silber, multiple publications in *Berichte der deutschen chemischen Gesellschaft* **30-38** (1900-1910) in particular *Chem. Ber.* **34** (1901) p. 2040 and **35** (1902) p. 1992.
- [2] A. P. Pelliccioli, J. Wirz, *Photochem. Photobiol. Sci.* **1** (2002), p. 441
- [3] J. Henzl, M. Mehlhorn, K. Morgenstern, *Nanotechnology* **18** (2007), p. 495502
- [4] G. C. R. Ellis-Davis, *Nature Methods* **4** (2007), p. 619
- [5] M. Takezaki, N. Hirota, M. Terazima, *J. Phys. Chem. A* **101** (1997), p. 3443
- [6] R. Hurley and A. C. Testa, *J. Am. Chem. Soc.* **90** (1968) p. 1951
- [7] R. W. Yip, D. K. Sharma, R. Giasson, D. Gravel, *J. Phys. Chem.* **88** (1984), p. 5770
- [8] S. Nagakura, M. Kojima, Y. Maruyama, *J. Mol. Spec.* **13** (1964), p. 174
- [9] K. Schaper, M. Etinski, T. Fleig, *Photochemistry and Photobiology* **85** (2009), 1075–1081
- [10] J. Mewes, A. Dreuw, J. Phys. Chem. A **15** (2013), p. 6691
- [11] A. Dreuw, M. Head-Gordon, *J. Am. Chem. Soc.* **126** (2004), p. 4007
- [12] A. Domenicano, G. Schultz, I. Hargittai, M. Colapietro, G. Portalone, P. George, C. W. Bock, *Struct. Chem.* **1** (1990), p. 107
- [13] M. Takezaki, N. Hirota, M. Terazima, *J. Phys. Chem. A* **108** (1998), p. 4685
- [14] M. Takezaki, N. Hirota, M. Terazima, H. Sato, T. Nakajima, S. Kato, *J. Phys. Chem. A* **101** (1997), p. 5190
- [15] J. Quenneville, M. Greenfield, D. S. Moore, S. D. McGrane, R. J. Scharff, *J. Phys. Chem. A* **115** (2011), p. 12286
- [16] H. Görner, *Photochem. Photobiol. Sci.* **4** (2005), p. 822
- [17] J. Kohl-Landgraf, F. Buhr, D. Lefrancois, J.-M. Mewes, H. Schwalbe, A. Dreuw, J. Wachtveitl, just accepted for publication in *J. Am. Chem. Soc.* DOI: 10.1021/ja410594y
- [18] T. Schmierer, F. Bley, K. Scharper, P. Gilch, *J. Photochem. Photobiol. A* **217** (2011), p. 363
- [19] M. A. El-Sayed, *J. Chem. Phys.* **38** (1963), p. 2834
- [20] A. T. B. Gilbert, N. A. Besley, P. M. W. Gill, *J. Phys. Chem. A* **112** (2008), p. 13164
- [21] J. F. Stanton, *J. Chem. Phys.* **101** (1994), p. 371
- [22] P. H. P. Harbach, M. Wormit, A. Dreuw, in preparation.
- [23] A. B Trofimov, G. Stelter, J. Schirmer, *J. Chem. Phys.* **111** (1999), p. 9982
- [24] A. I. Krylov, P. M. W. Gill, *WIREs Comput Mol Sci* **3** (2013), p. 317
- [25] F. Neese, *WIREs Comput. Mol. Sci.* **2** (2012), p. 73
- [26] R. Ahlrichs, M. Bär, M. Häser, H. Horn and C. Kölmel, *Chem. Phys. Lett.* **162** (1989), p. 165
- [27] S. Grimme and M. Waletzke, *J. Chem. Phys.* **111**, (1999) p. 5645
- [28] M. Kleinschmidt, C. M. Marian, S. Grimme, M. Waletzke, *J. Chem. Phys.* **130**, (2009), p. 44708
- [29] M. Kleinschmidt and J. Tatchen and C. M. Marian, *J. Comp. Chem.* **23**, (2003) p. 824
- [30] M. Kleinschmidt, C. M. Marian, *Chem. Phys.* **311** (2005), p. 71
- [31] F. Weigend and R. Ahlrichs, *Phys. Chem. Chem. Phys.* **7** (2005), p. 3297
- [32] T.H. Dunning Jr., *J. Chem. Phys.* **90** (1989), p. 1007
- [33] T. Elsaesser, W. Kaiser, *Annu. Rev. Phys. Chem.* **42** (1991), p. 83
- [34] M. Pabst, A. Köhn, J. Gauss, J. F. Stanton, *Chem. Phys. Lett.* **495** (2010), p. 135